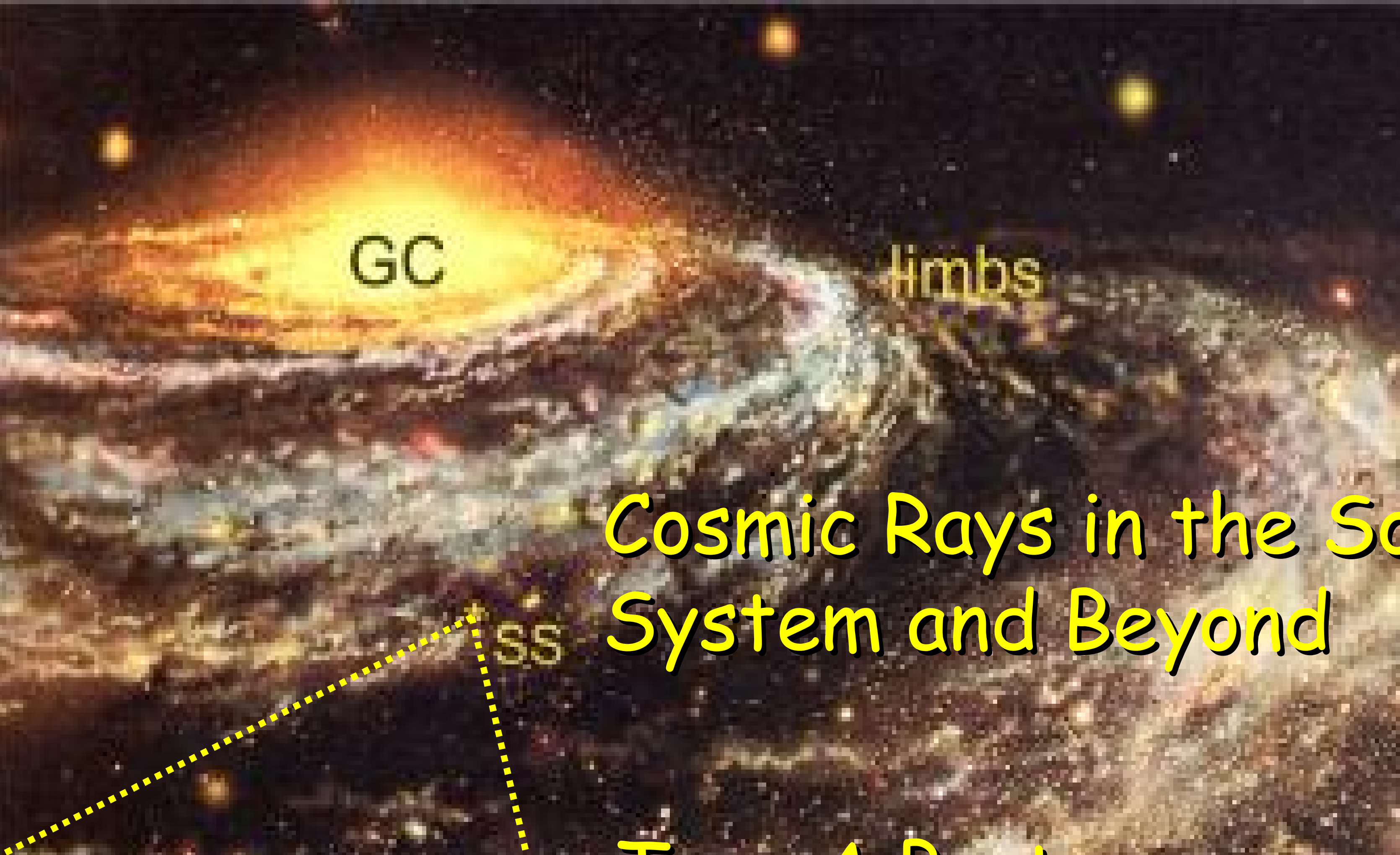

Cosmic Rays in the Solar System and Beyond

Troy A Porter

University of California, Santa Cruz
Santa Cruz Institute for Particle Physics

All Particle CR Spectrum

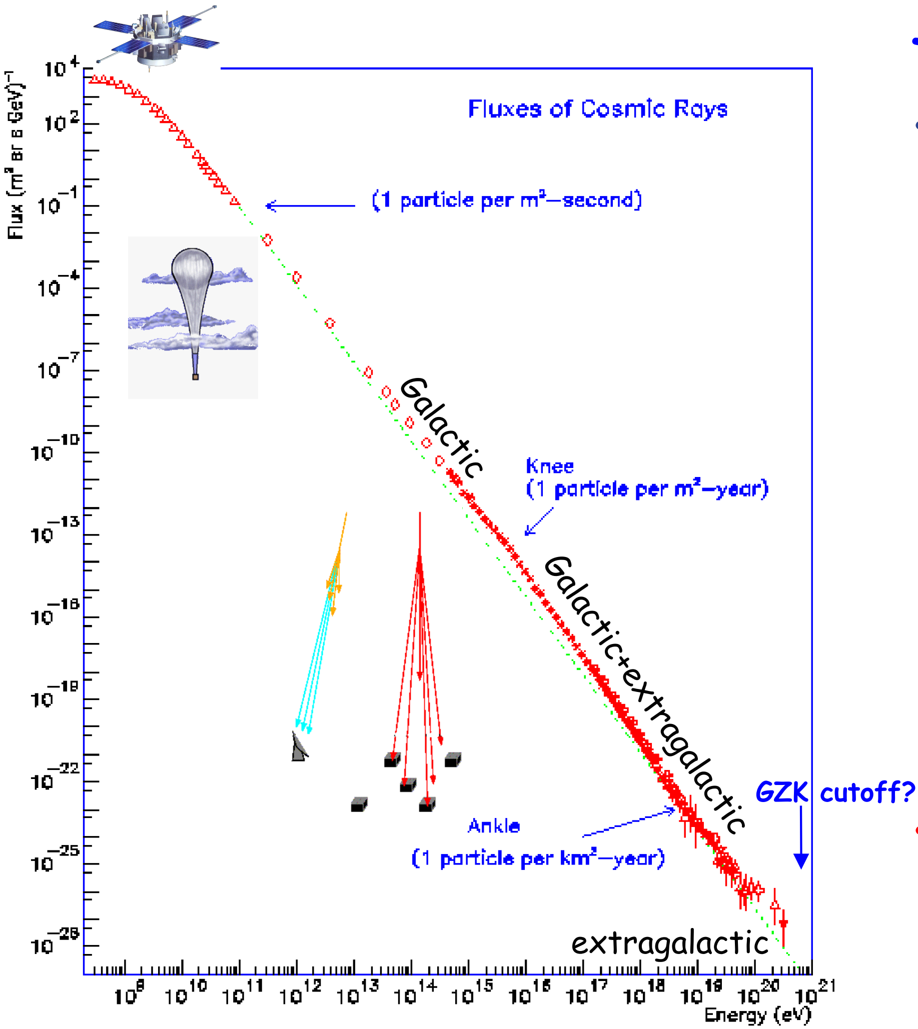

This is an astonishing observation!

- All particle CR spectrum is almost featureless:
  - -the knee
  - -the ankle
  - -GZK cutoff

  These are the only features in >12 decades in energy and >32 decades in intensity!

  However, there is a lot of information hidden in the spectra and abundances of individual CR species: nuclear isotopes, antiprotons, electrons, positrons (+diffuse gamma rays)
- All of physics is involved: various branches of Astrophysics, MHD, shock waves, plasma physics, atomic, nuclear, & particle physics, exotic physics – SUSY…
- CRs are the only direct probes of the interstellar material available to us.

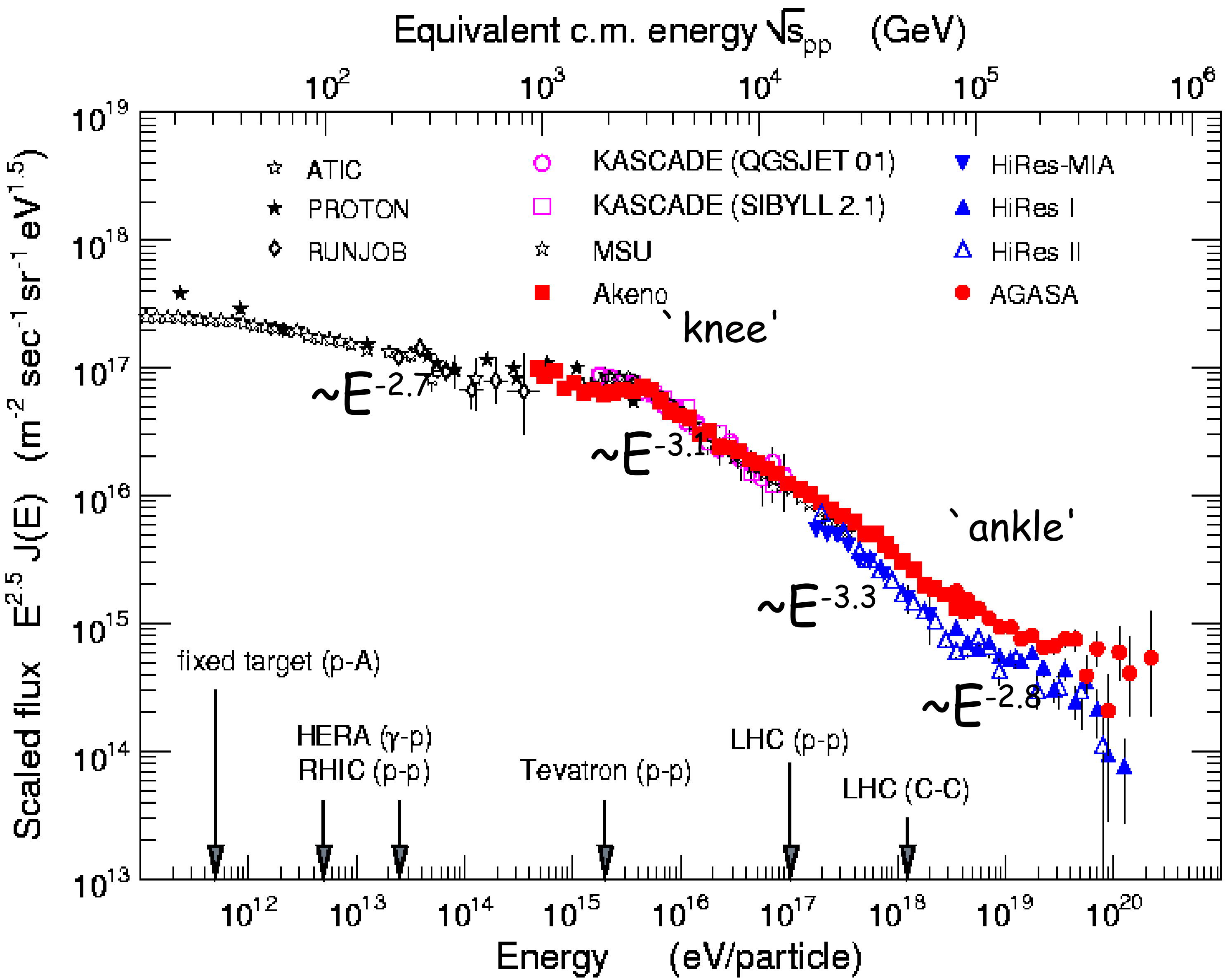

Equivalent c.m. energy $\sqrt{s_{pp}}$ (GeV)
10^2 10^3 10^4 10^5 10^6
ATIC
PROTON
RUNJOB
KASCADE (QGSJET 01)
KASCADE (SIBYLL 2.1)
MSU
Akeno
HiRes-MIA
HiRes I
HiRes II
AGASA
`knee'
~E$^{-2.7}$
~E$^{-3.1}$
`ankle'
~E$^{-3.3}$
~E$^{-2.8}$
fixed target (p-A)
HERA (γ-p)
RHIC (p-p)
Tevatron (p-p)
LHC (p-p)
LHC (C-C)
Scaled flux E$^{2.5}$ J(E) (m^{-2} sec^{-1} sr^{-1} eV$^{1.5}$)
10^{13} 10^{14} 10^{15} 10^{16} 10^{17} 10^{18} 10^{19}
10^{12} 10^{13} 10^{14} 10^{15} 10^{16} 10^{17} 10^{18} 10^{19} 10^{20}
Energy (eV/particle)

CR propagation: the Milky Way galaxy

Optical image: Cheng et al. 1992, Brinkman et al. 1993
Radio contours: Condon et al. 1998 AJ **115**, 1693

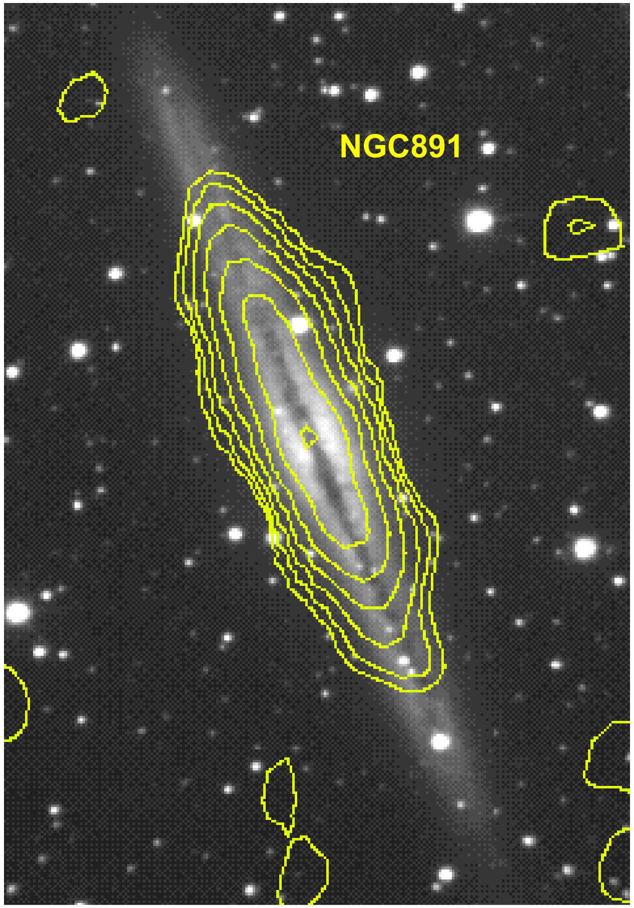

R Band image of NGC891
1.4 GHz continuum (NVSS), 1,2,…64 mJy/ beam

1 pc ~ 3×10^{18} cm

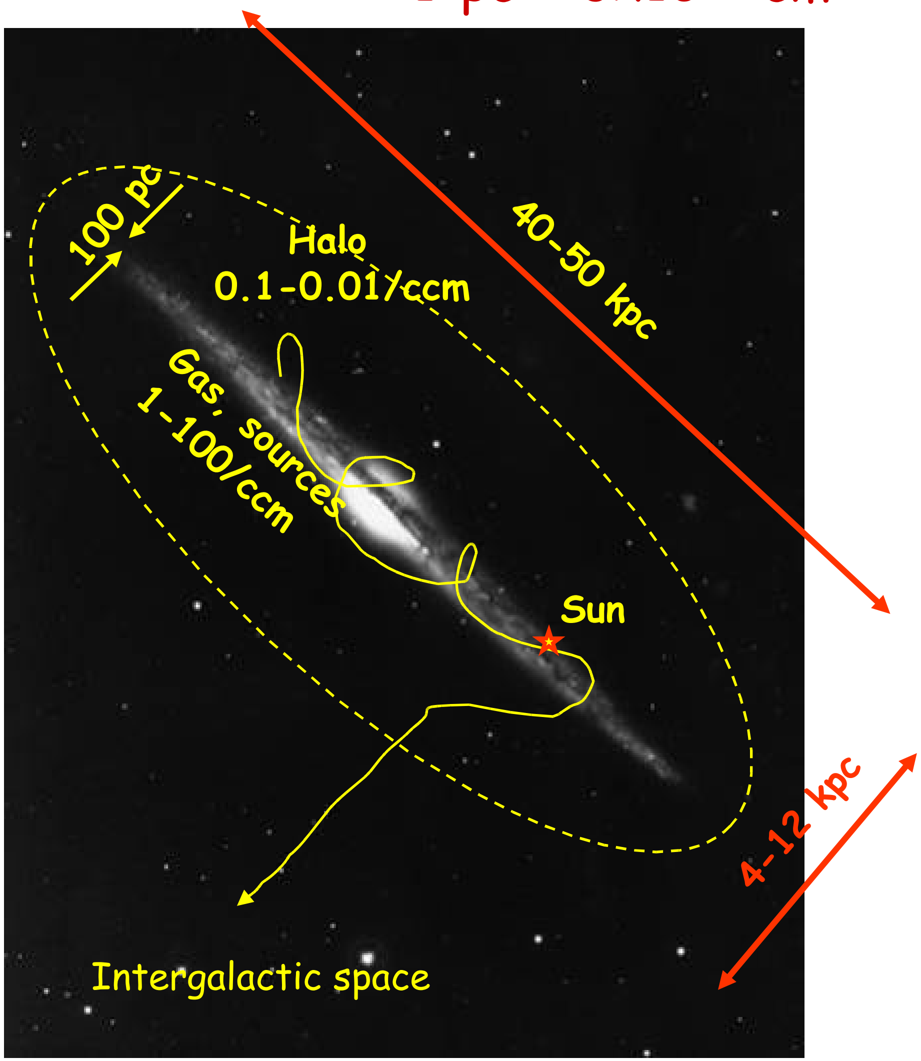

"Flat halo" model (Ginzburg & Ptuskin 1976)

Fermi LAT Project

CR Interactions in the Interstellar Medium

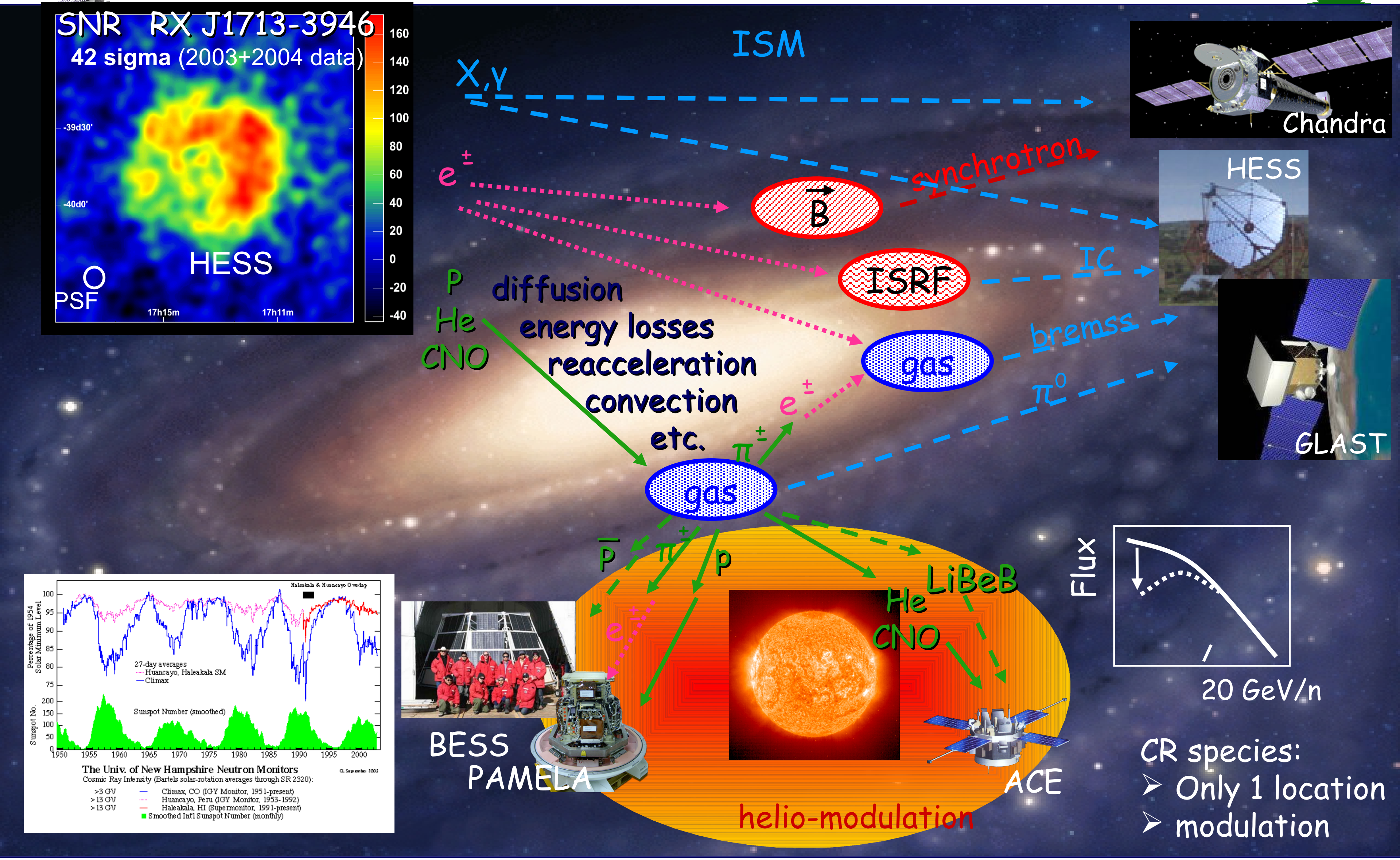

Nuclear component in CR: What we can learn?

Stable secondaries:
Li, Be, B, Sc, Ti, V

Radio ($t_{1/2}$~1 Myr):
^{10}Be, ^{26}Al, ^{36}Cl, ^{54}Mn

K-capture: ^{37}Ar, ^{49}V, ^{51}Cr, ^{55}Fe, ^{57}Co

Short $t_{1/2}$ radio ^{14}C & heavy Z>30

Heavy Z>30:
Cu, Zn, Ga, Ge, Rb

Propagation parameters:
Diffusion coeff., halo size, Alfvén speed, convection velosity…

Energy markers:
Reacceleration, solar modulation

Local medium:
Local Bubble

Material & acceleration sites, nucleosynthesis (r-vs. s-processes)

Nucleo-synthesis: supernovae, early universe, Big Bang…

Dark Matter $(\bar{p},\bar{d},e^+,\gamma)$

Extragalactic diffuse γ-rays: blazars, relic neutralino

Solar modulation

Fermi LAT Project

CR and γ-ray instruments

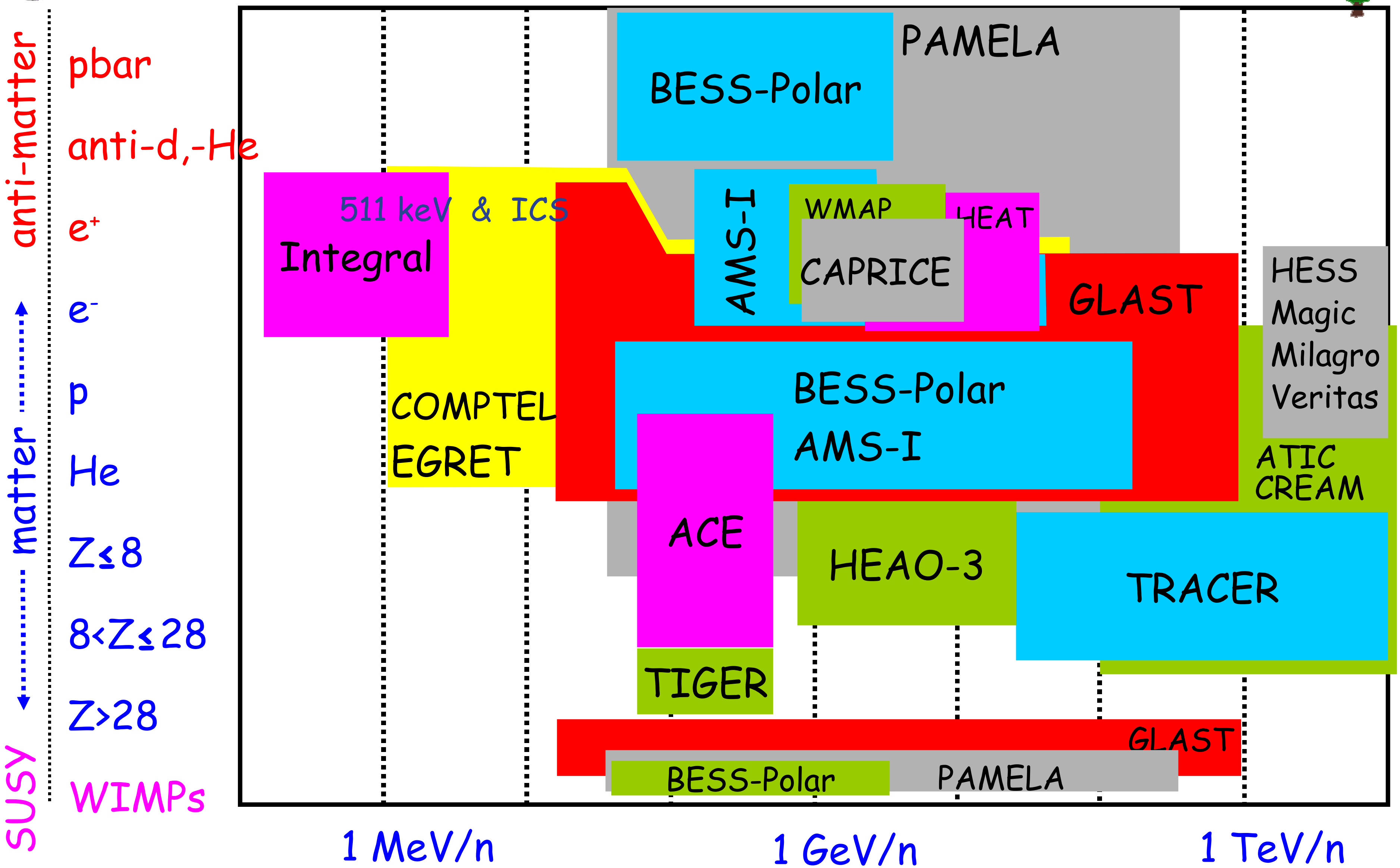

PaMeLa a Payload for Antimatter Matter Exploration and Light-nuclei Astrophysics

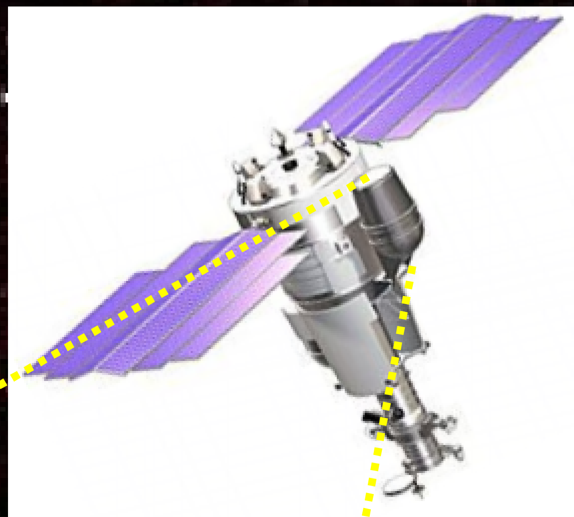

Direct vs Indirect Measurements of CRs

- Direct measurements from deep inside heliosphere
  - Good data < 200 GeV/nuc, even less < 30 GeV/nuc
- Indirect via observations of radio, X-, γ-rays produced by p, α, $e^{\pm}$, etc. during propagation in ISM
- e^{+} observed through annihilation + IC + radio
- γ-ray instruments probe CR energies much higher than the observed γ-ray energies
  - IACTs (E_{γ}>100 GeV) → E_{CR} ~ TeV energies
  - Fermi (20 MeV<E_{γ}<~100s GeV) → E_{CR} < 1 TeV comparable to some direct measurements (PAMELA, PPB-BETS)
- Indirect measurements provide snapshot, direct measurements average of 10s Myr in ISM and kpc scales
- Big issue is connecting what we see deep in heliosphere to IS space → Fermi-LAT will provide first way of doing this!
- To understand DM, CMB studies, need to understand CRs

Cosmic rays in the heliosphere

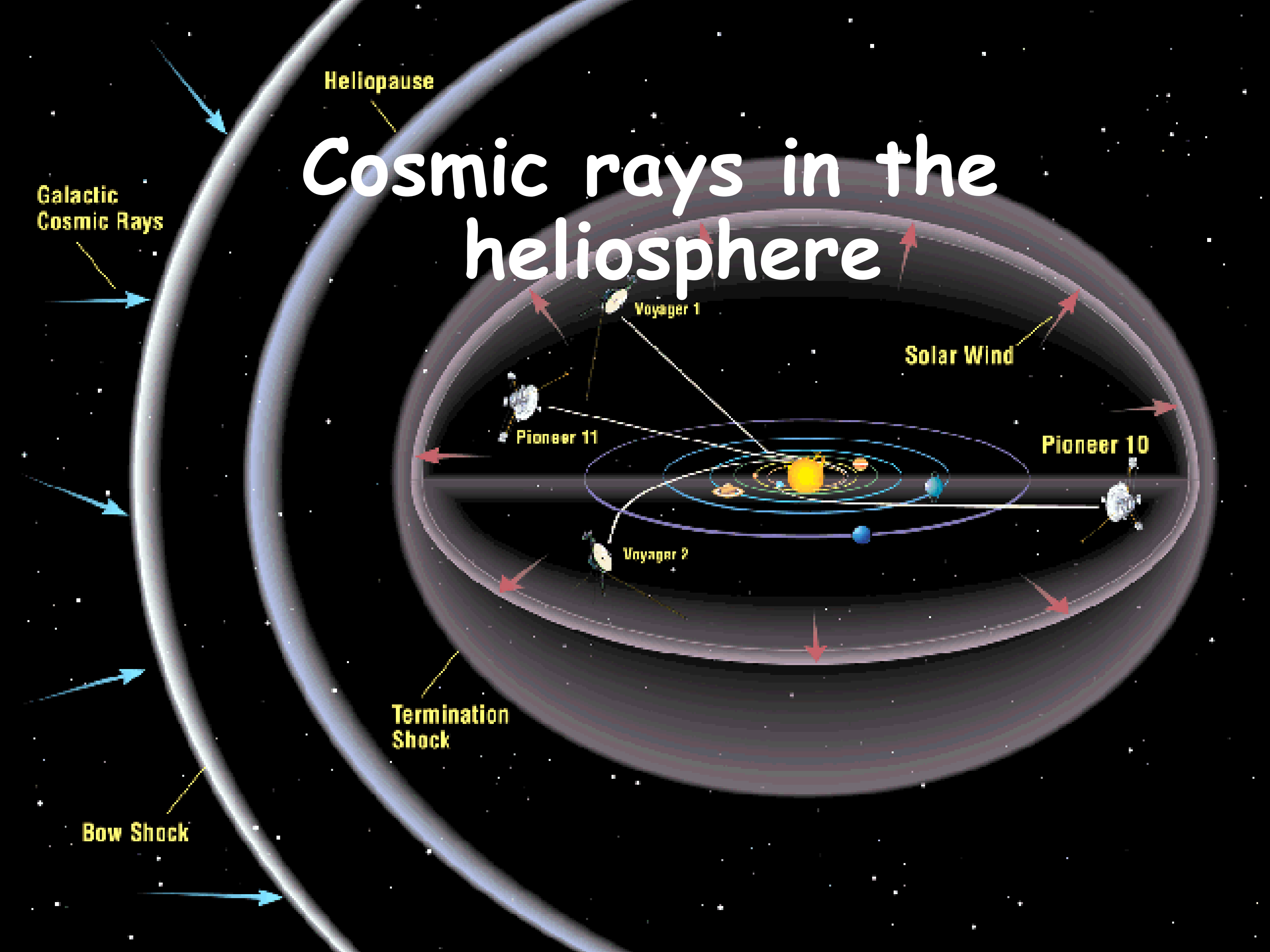

Inverse Compton scattering

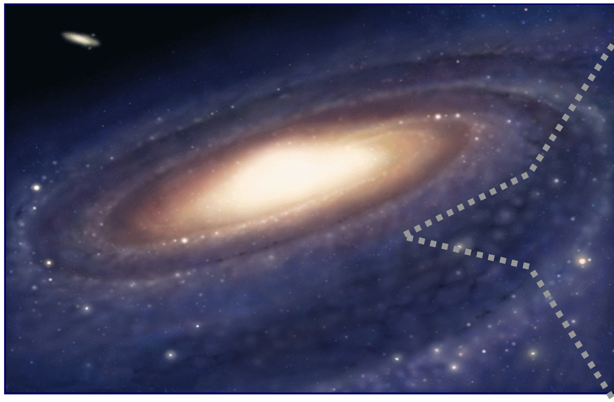

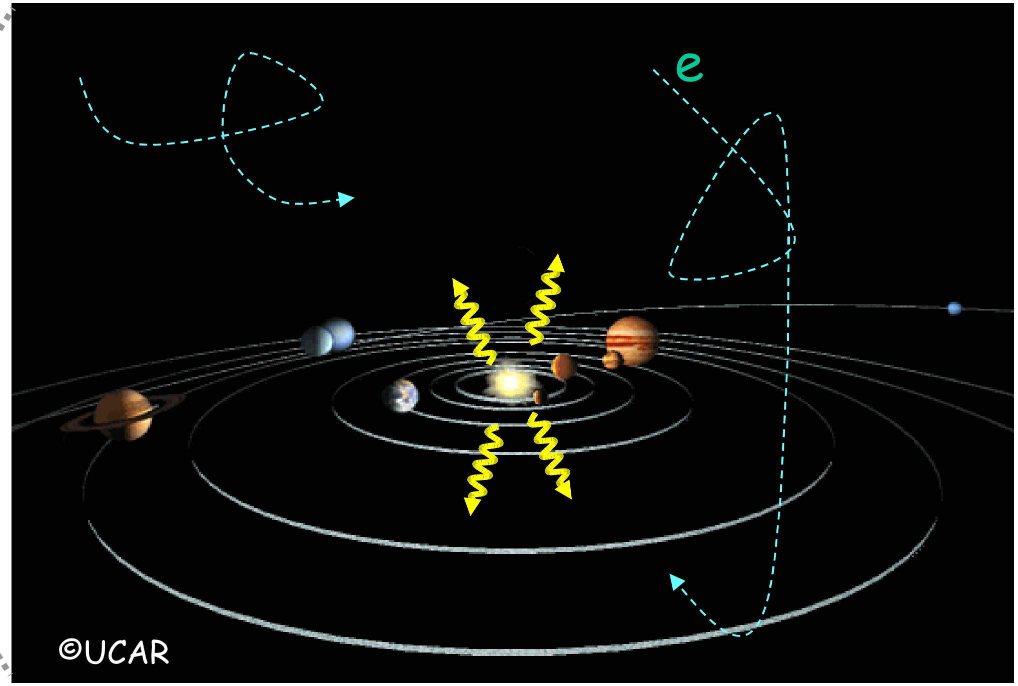

Inverse Compton scattering

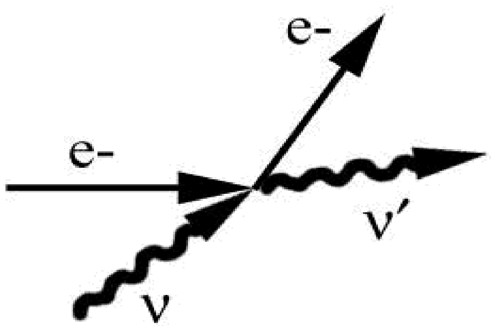

$\nu' > \nu$

High energy e- initially

e- loses energy

The heliosphere is filled with Galactic CR electrons and solar photons

- electrons are isotropic
- photons have a radial distribution with outward direction

Anisotropic effect on solar photons

$$\frac{dF_\gamma}{d\epsilon_2} = \frac{1}{4}\int_L dx\, \frac{R_\odot^2}{r^2} \int d\gamma_e \frac{dJ_e(r,\gamma_e)}{d\gamma_e} \times \int d\epsilon_1 \frac{dn_{bb}(\epsilon_1, T_\odot)}{d\epsilon_1} \frac{dR(\gamma_e,\epsilon_1)}{d\epsilon_2}$$

e

Head-on collision:

$E_\gamma \sim \gamma_e^2 \nu_{bb}$

10 GeV e → 100 MeV γs

Target photons:

$\rho = 0.25 n_{bb} (R_S/r)^2$

$T_{bb} = 5770$ K

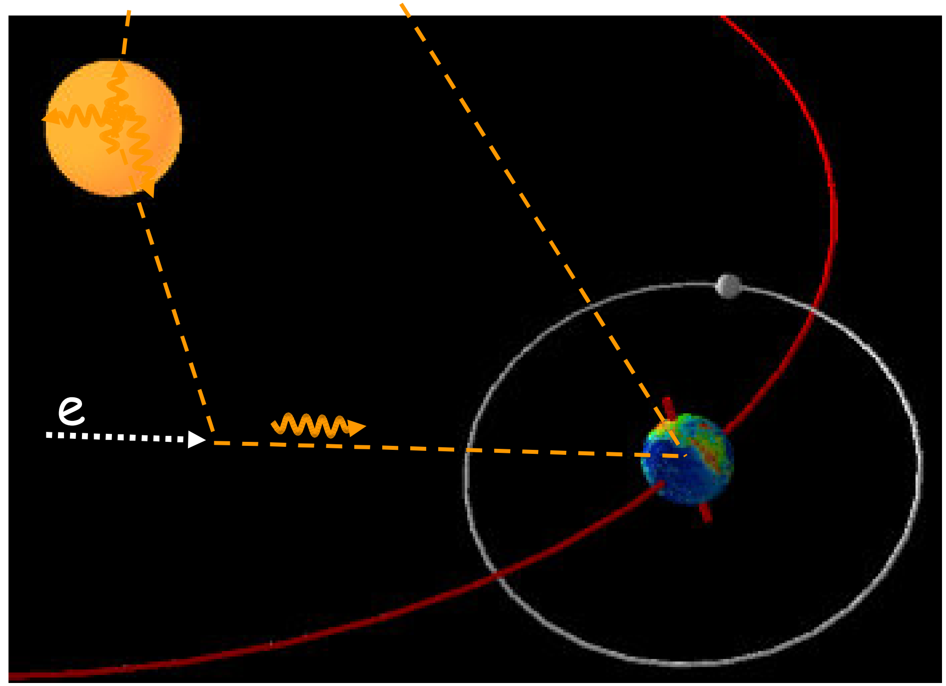

Following collision:

$E_\gamma \sim (1/\gamma)\gamma\nu_{bb} \sim \nu_{bb}$

Inner Heliospheric Probe

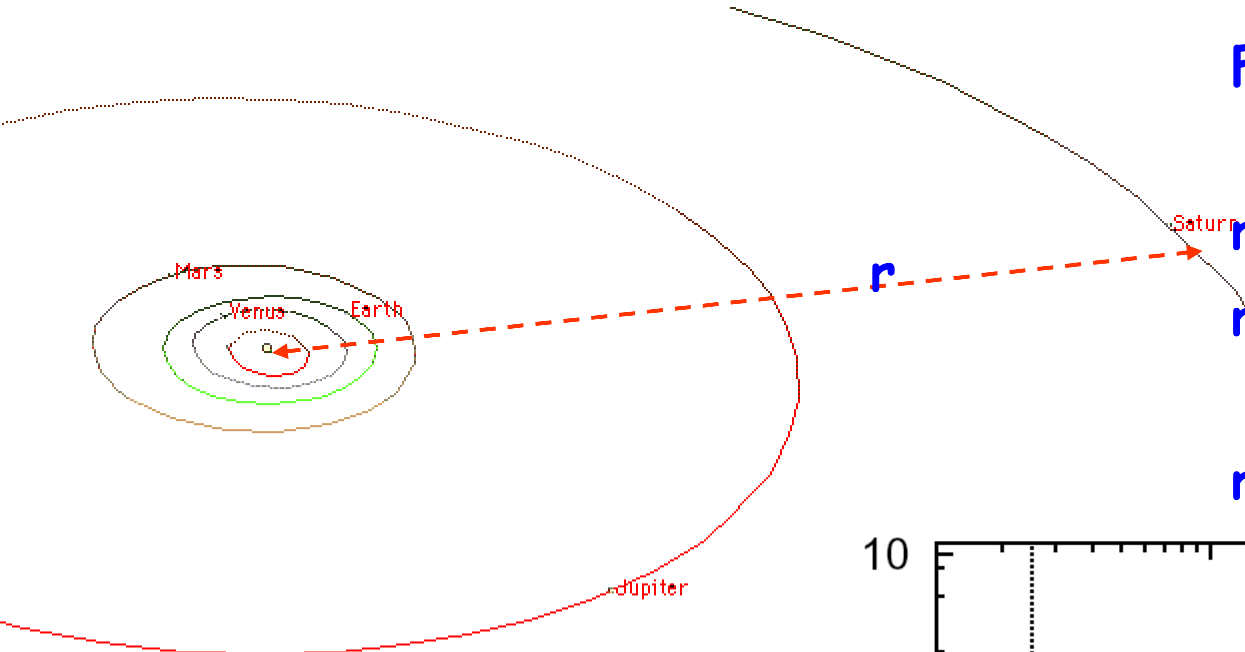

$\mathrm{Flux}_{IC} \sim 1/r$

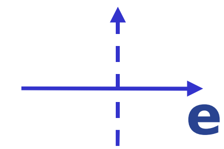

$r_1\ (AU) = \sin\theta, \quad \theta<90°$

$r_1\ (AU) = 1, \quad \theta>90°$

$r_2 = 10 r_1$

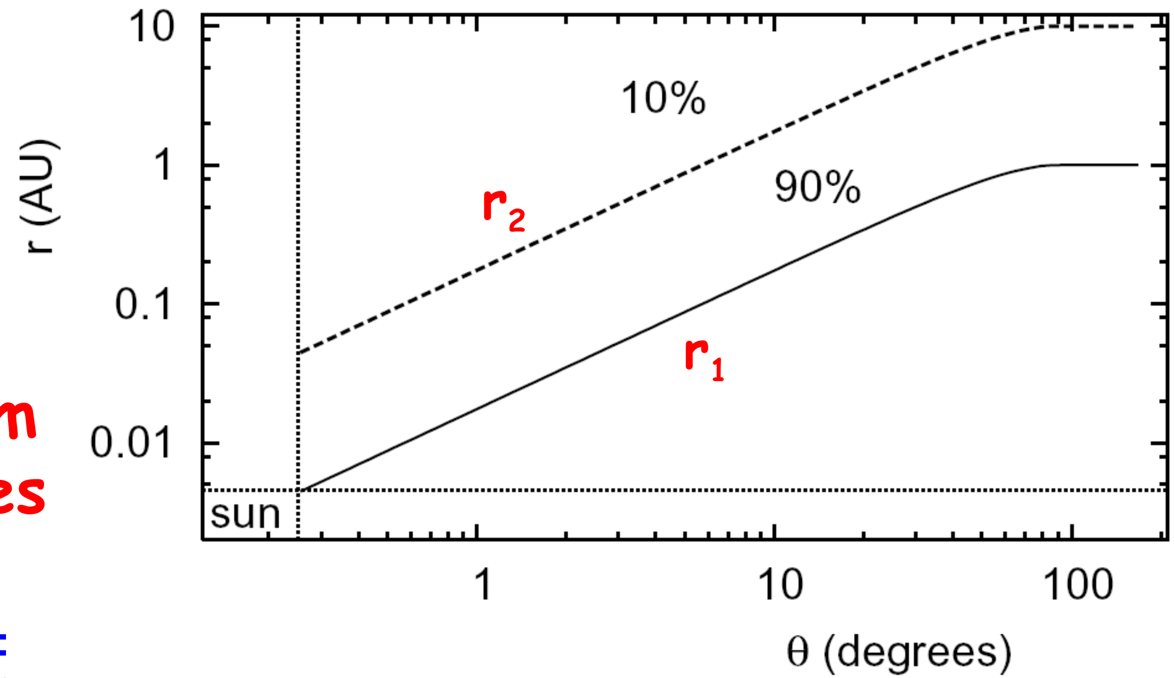

Looking in different directions one can probe the e-spectrum at different distances from the Sun!

The Ecliptic

Averaged over one year, the ecliptic will be seen as a stripe on the sky, but the emission comes from all directions

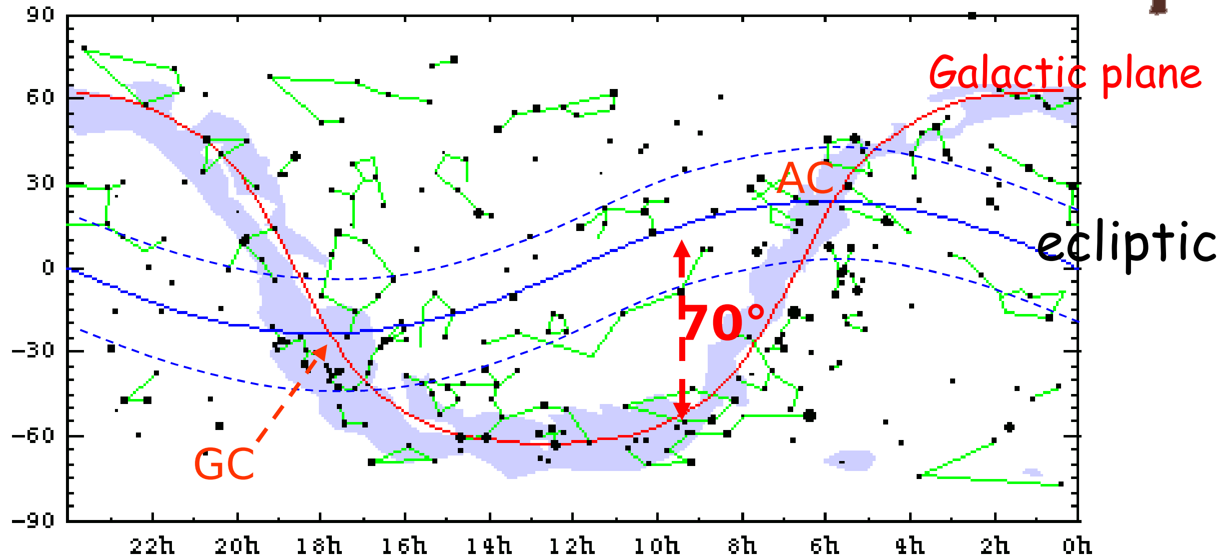

Integral Intensity

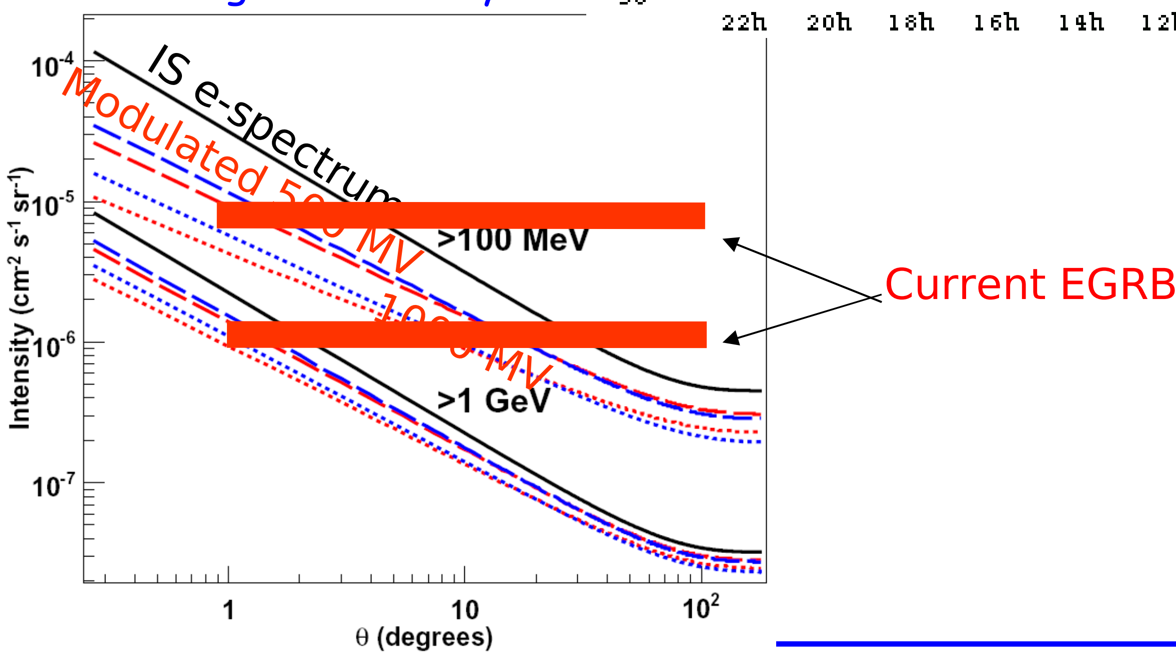

Differential Spectrum

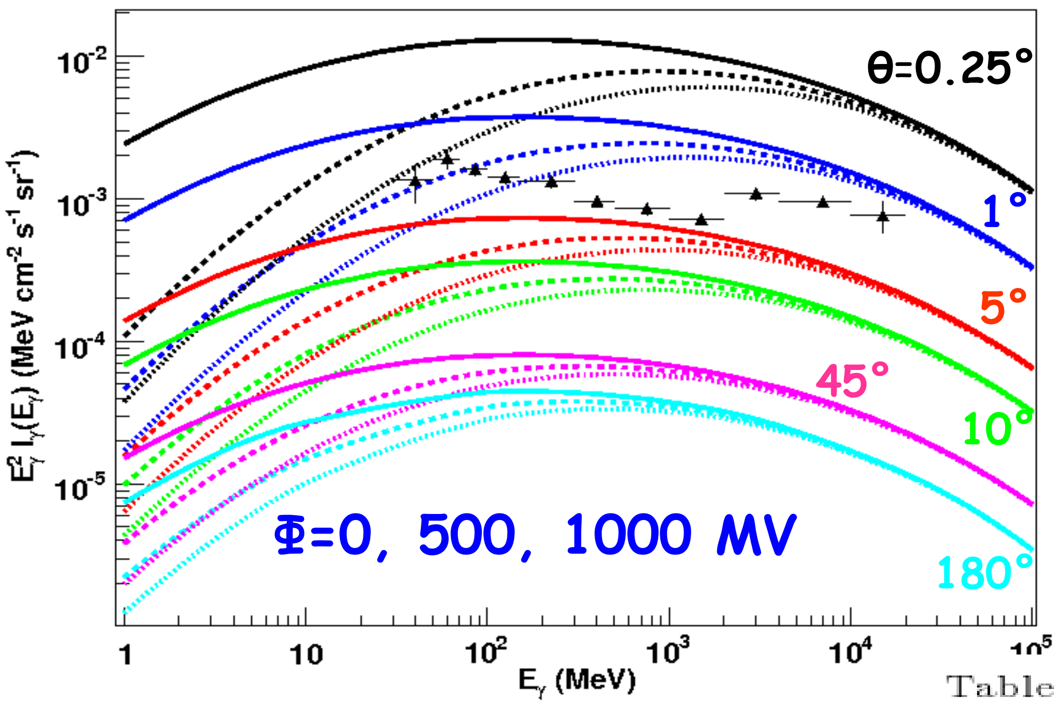

IC spectrum < 1 GeV shows strong dependence on the modulation level

→ variations of γ-ray flux over the solar cycle

IC integral flux

F(>100 MeV, θ<2.5°) ~ 2×10^{-7} cm^{-2} s

EGRET upper limit = 2×10^{-7} cm^{-2} s^{-1}

Table 1. All-sky average integral intensity

E	$\Phi_0 = 0$	500 MV	1000 MV
>10 MeV	6.6	3.9	2.7
>100 MeV	0.8	0.7	0.5
>1 GeV	0.06	0.05	0.05

Note. — Units 10^{-6} cm^{-2} s^{-1} sr^{-1}.

Found in EGRET data!

Thompson et al. 1997:
Upper limit $2x10^{-7}$ cm^{-2} s^{-1}

Reanalysis by Orlando, Petry, Strong 2007:

Discovery of both solar disk albedo emission and extended inverse Compton-scattered radiation in combined analysis of EGRET data from June 1991!!

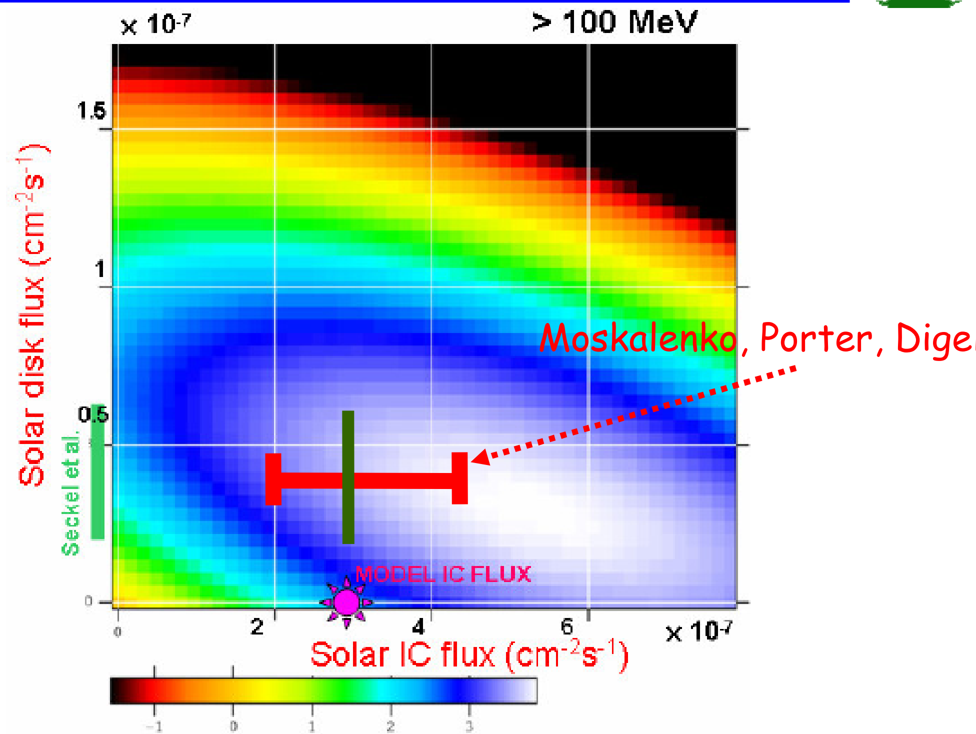

FIGURE 1. Log Likelihood above 100 MeV as function of the solar disk flux and extended solar flux, relative to point at (0,0). The level of our predicted IC model flux and the predicted disk flux [7] are shown.

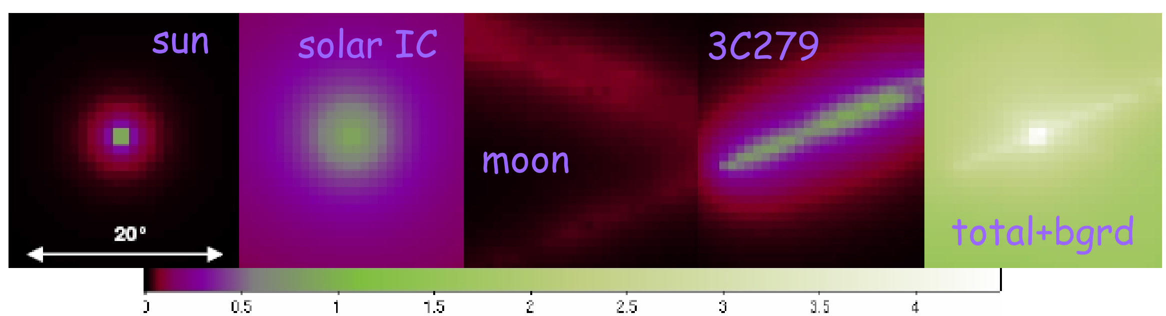

FIGURE 2. Fitted model counts of the main components centered on the Sun. From left to right: Sun disk, Sun IC, moon, 3C 279, and the total predicted counts including uniform background. The colors show the counts/pixel, for 0.5°× 0.5° pixels.

EGRET Observations of the Moon

THOMPSON ET AL.: GAMMA RAY OBSERVATIONS OF THE MOON AND QUIET SUN

Table 1. EGRET Viewing Periods for Observations of the Moon

Viewing Period	Start	End	l	b	Neutron Monitor, cts/(hr/100)
0110	Oct. 5, 1991 0925	Oct. 9, 1991 1330	294.25	63.67	2023
0190	Feb. 2, 1992 2109	Feb. 6, 1992 1514	58.15	−43.00	2068
0400	Sept. 22, 1992 0840	Sept. 25, 1992 1615	195.90	44.71	2246
3070	Nov. 9, 1993 1347	Nov. 12, 1993 0230	268.69	69.24	2336
3170	Feb. 17, 1994 1600	Feb. 19, 1994 1034	158.48	−45.38	2294
3200	March 9, 1994 2030	March 14, 1994 1345	83.09	−45.47	2244
4050	Nov. 29, 1994 1527	Dec. 1, 1994 0915	306.67	56.54	2319
4070	Dec. 25, 1994 0940	Dec. 29, 1994 0245	334.33	62.98	2340

Here, l is galactic longitude; b is galactic latitude.

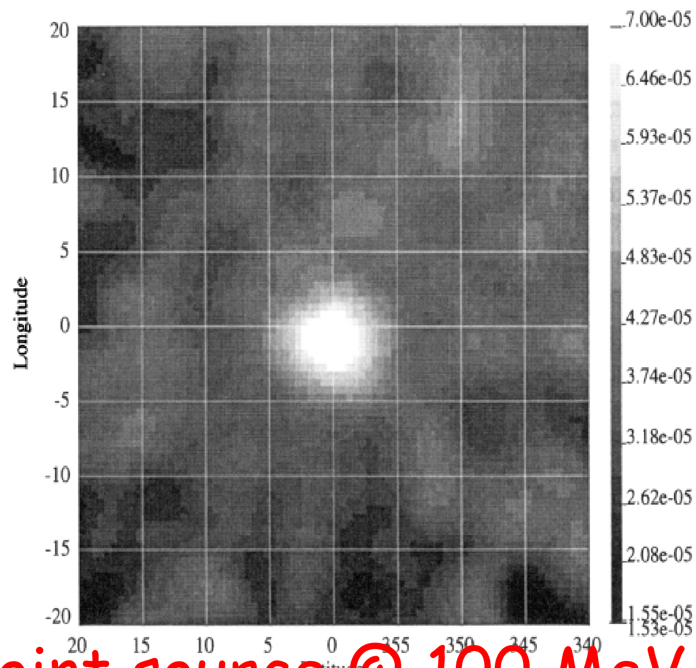

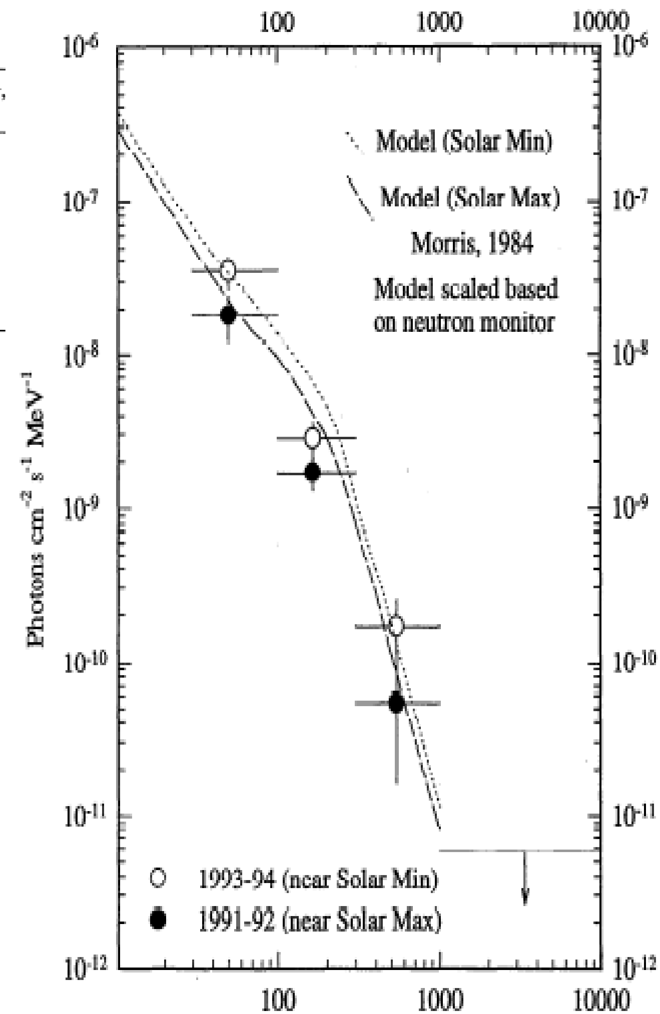

Point source @ 100 MeV

~200 γ-rays >100 MeV

Moon Gamma-Ray Albedo

Fermi LAT Project

Kinematics of the interaction:

- Cascades develop into surface → high energy γ-rays from tangent to surface
- Splash pions are low-energy and decay at "rest"

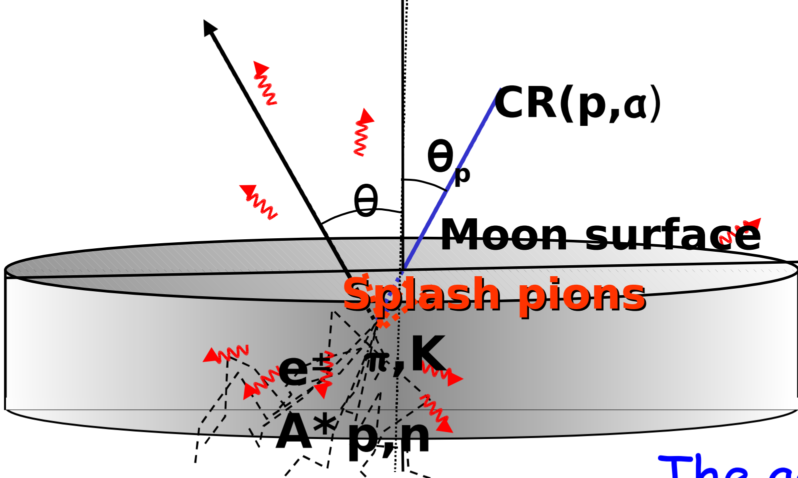

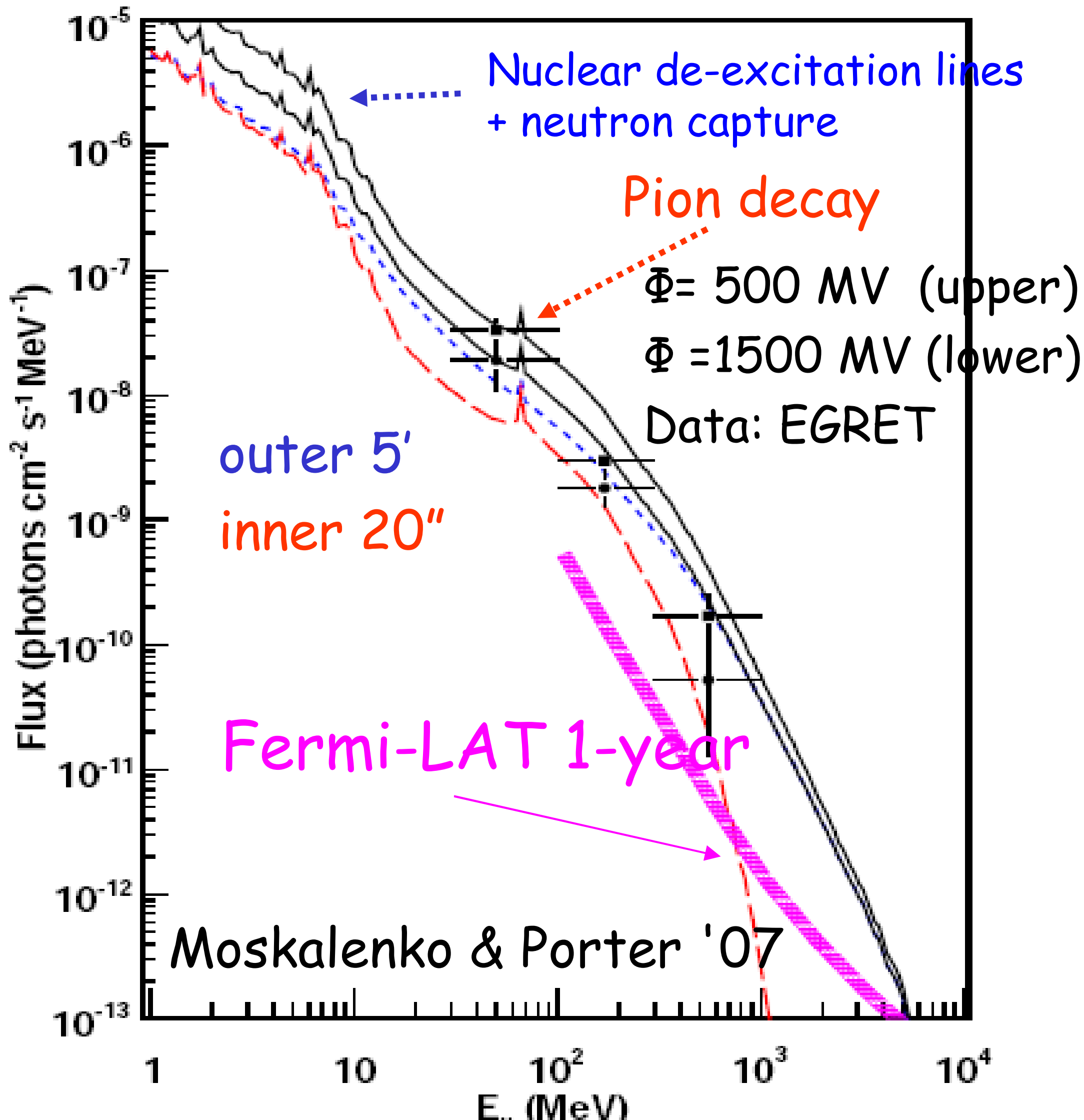

The agreement is remarkable: no free parameters

Fermi LAT Project

A Zoo of Small Solar System Bodies

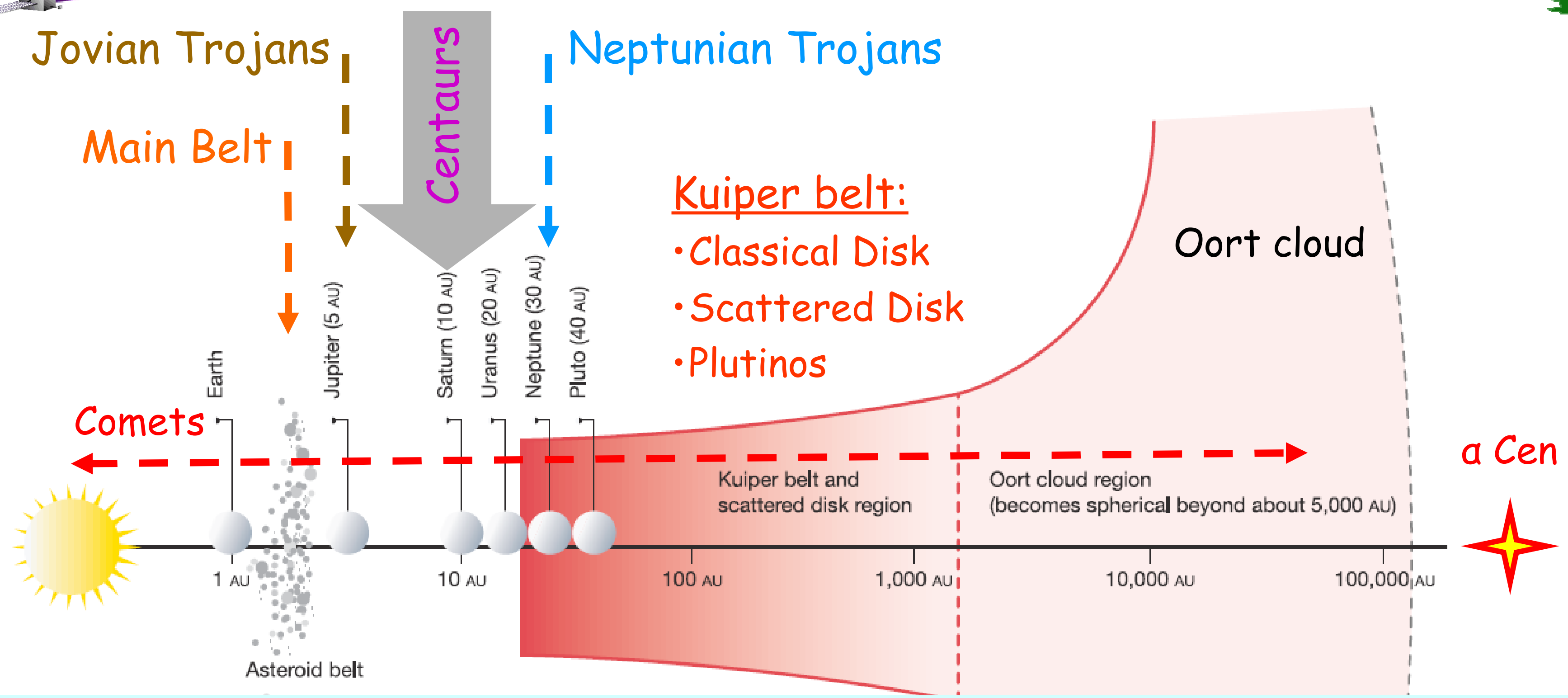

Table 1 **The primary cometary reservoirs of the Solar System**

	Kuiper belt	Oort cloud
Shape	Disk-like	Spheroidal
Distance range	30–1,000 AU	1×10^3–1×10^5 AU
Comet population	$\sim$5–10×10^9	1×10^{11}–5×10^{12}
Estimated mass (including smaller debris)	$\sim0.1\ M_\oplus$	1–50 $M_\oplus$
Ambient surface temperatures	30–60 K	5–6 K
Origin	Largely *in situ*	Ejected material from the Kuiper belt and outer-planets zone
Return mechanism from the reservoir	Dynamical chaos due to planetary perturbations and collisions	Perturbations due to passing stars, galactic tides and molecular clouds

Stern'03

Hot Topics

- Formation and evolution of the planetary system and exo-solar planetary systems
  - 1992 (Jewitt & Luu) – first object beyond Neptune since Pluto
  - 2004, 2005 (Sheppard & Trujillo) – discovery of Neptunian Trojans (L4); L5 is currently in the direction of the GC
  - Ejection of material into distant eccentric orbits (Oort cloud)
  - Orbital precession (expansion/contraction) of the giant planets and SSSB families (Neptune: 20 AU -> 30 AU; Kuiper belt)
- The number of small solar system bodies in different dynamic families and their size distribution
  - Formation of planetesimals
  - Pristine material
  - "Freeze-in" capture (Trojans)
- Probe of interstellar spectrum of CR protons + He

SSSB Size Distributions

2. SMALL SOLAR SYSTEM BODIES

The asteroid mass and size distributions are thought to be governed by collisional evolution and accretion. Collisions between asteroids give rise to a cascade of fragments, shifting mass toward smaller sizes, while a small body impact with a much larger asteroid leads to the growth of the latter. The first comprehensive analytical description of such a collisional cascade is given by Dohnanyi (1969). Under the assumptions of scaling of the collisional response parameters and an upper cutoff in mass, the relaxed size and mass distributions approach power-laws:

$$dN = am^{-k}dm \qquad (1)$$

$$dN = br^{-n}dr, \qquad (2)$$

where m is the asteroid mass, r is the asteroid radius, and a, b, k, n are constants. These equilibrium distributions extend over all size and mass ranges of the population except near its high-mass end. The constants in eqs. (1),

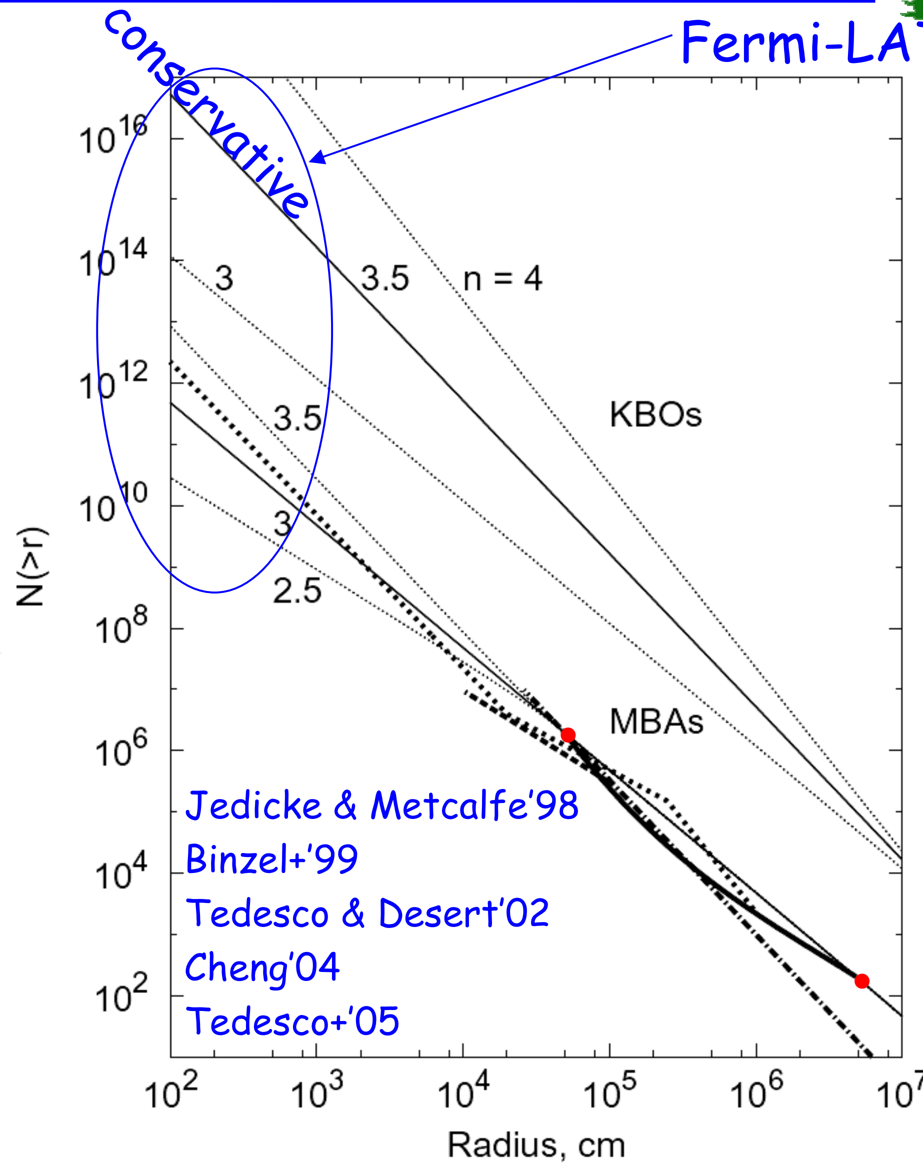

- Collisional evolution & accretion
- Relaxed size distribution n=3.5 (assuming scaling of collisional response parameters)
- Scaling breaks…

Albedo of SSSBs

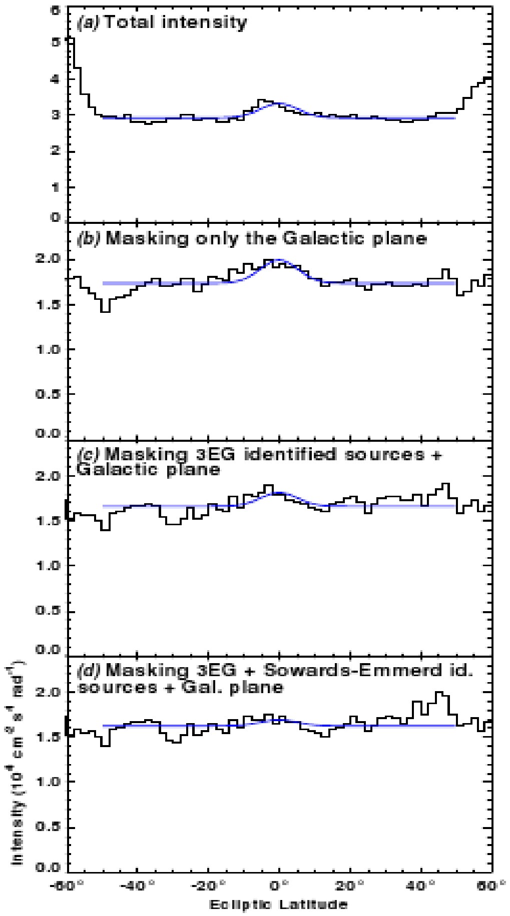

FIG. 5.— Profiles of γ-ray intensity with β derived from EGRET data as described in the text. The energy range is 100–500 MeV and the profiles have been averaged over all ecliptic longitudes. (*a*) Profile derived with no masking of Galactic diffuse emission or γ-ray point sources. (*b*) Profile with the Galactic plane ($|b| < 10°$ for $|l| > 90°$ and $|b| < 20°$ for $|l| < 90°$) excluded. (*c*) Profile with the identified 3EG sources (Hartman et al. 1999) and the Galactic plane excluded. (*d*) Profile with the identified 3EG sources plus the further blazar identifications proposed by Sowards-Emmerd (2003, 2004) excluded. Overlaid on each profile is the best-fitting gaussian (12.5° FWHM, centered on $\beta = 0$) plus a constant, fit for the region $|\beta| < 50°$. This approximates the distribution of albedo γ-ray emission expected for the the KBO.

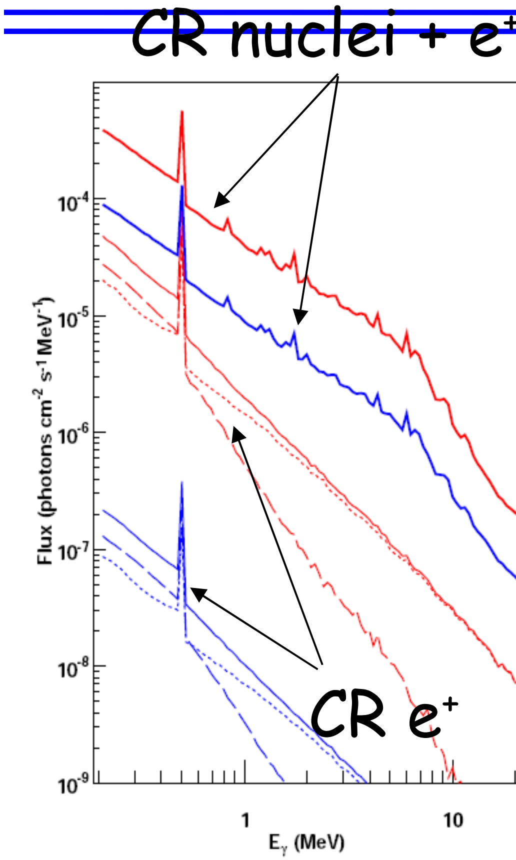

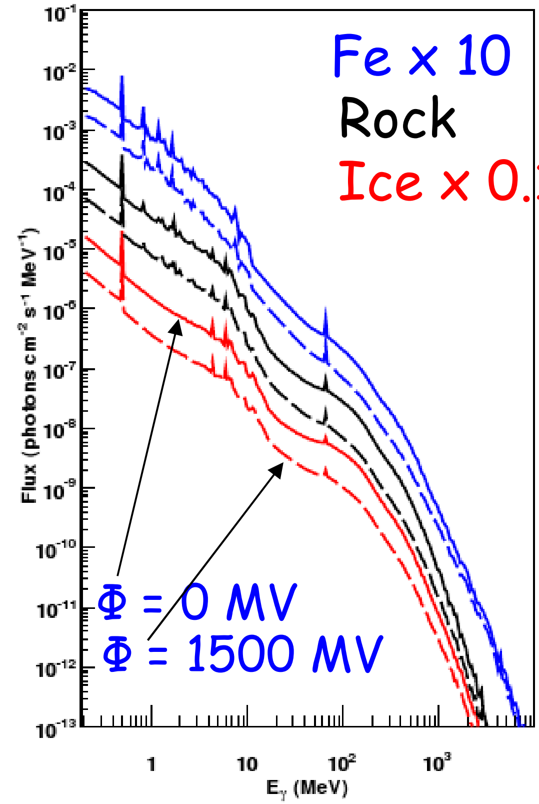

TABLE 1. DIFFUSE INTENSITY AROUND THE ECLIPTIC (100–500 MEV)

Set of cuts	$\|\beta\| < 15°$			
in Figure 5	Flux, cm^{-2} s^{-1}	Stat. error	Fitted flux, cm^{-2} s^{-1}	Stat. error
a	1.006×10^{-5}	5.5×10^{-7}	9.16×10^{-8}	3.5×10^{-7}
b	7.95×10^{-8}	5.8×10^{-7}	5.95×10^{-8}	3.7×10^{-7}
c	3.59×10^{-8}	6.7×10^{-7}	3.53×10^{-8}	4.4×10^{-7}
d	1.1×10^{-7}	7.4×10^{-7}	1.52×10^{-8}	5.1×10^{-7}

Moskalenko, Porter, Digel, Michelson, & Ormes ApJ 681, 1708 (2008)

Albedo of SSSBs

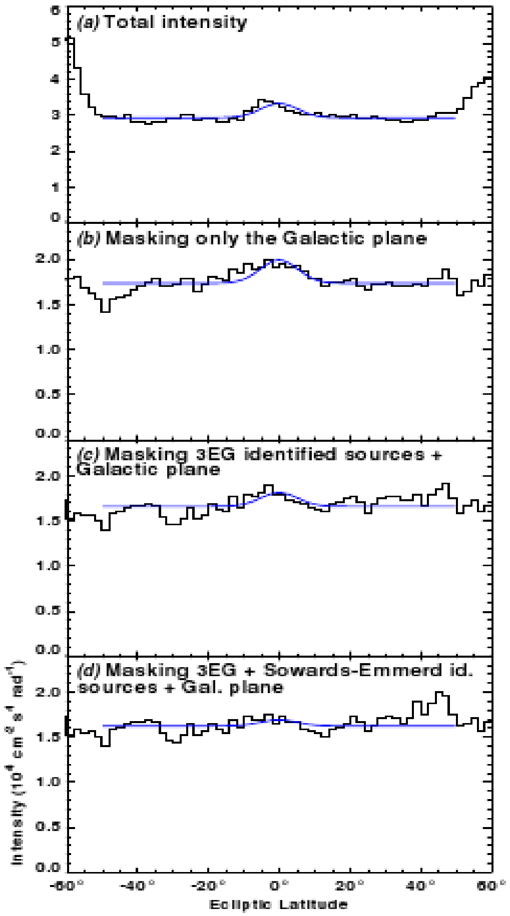

FIG. 5.— Profiles of γ-ray intensity with β derived from EGRET data as described in the text. The energy range is 100–500 MeV and the profiles have been averaged over all ecliptic longitudes. (a) Profile derived with no masking of Galactic diffuse emission or γ-ray point sources. (b) Profile with the Galactic plane ($|b| < 10°$ for $|l| > 90°$ and $|b| < 20°$ for $|l| < 90°$) excluded. (c) Profile with the identified 3EG sources (Hartman et al. 1999) and the Galactic plane excluded. (d) Profile with the identified 3EG sources plus the further blazar identifications proposed by Sowards-Emmerd (2003, 2004) excluded. Overlaid on each profile is the best-fitting gaussian (12.5° FWHM, centered on $\beta = 0$) plus a constant, fit for the region $|\beta| < 50°$. This approximates the distribution of albedo γ-ray emission expected for the the KBO.

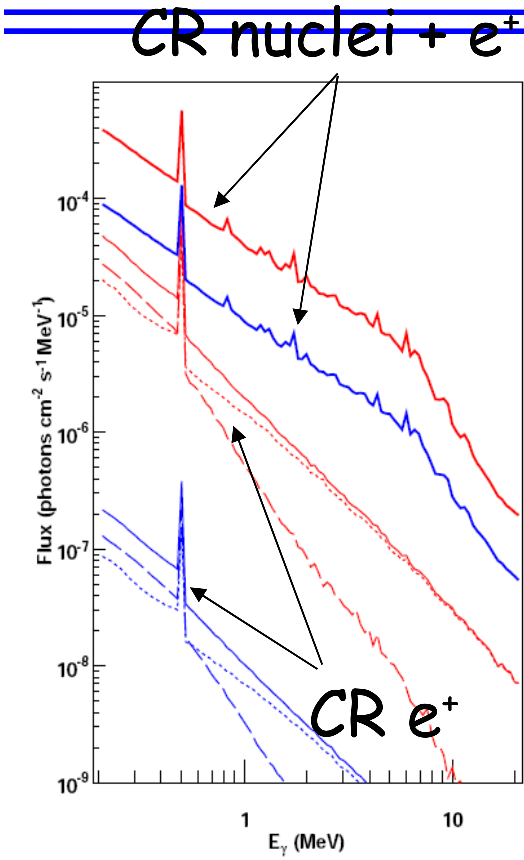

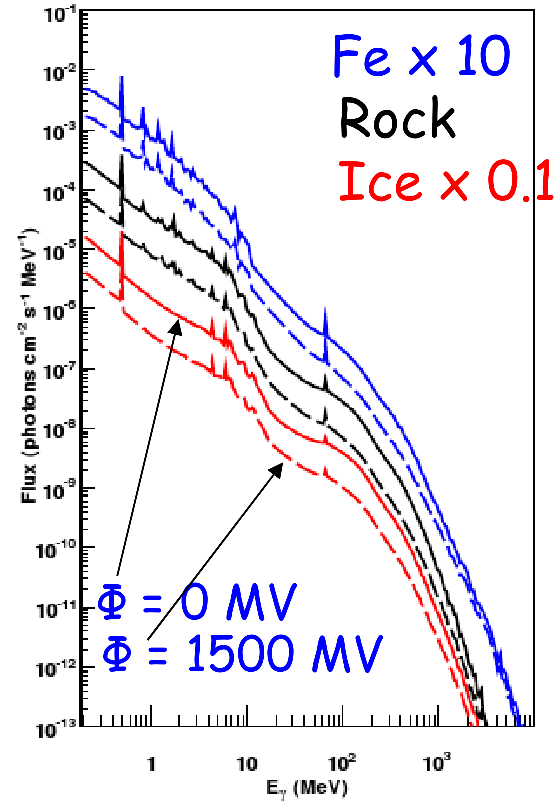

TABLE 1. DIFFUSE INTENSITY AROUND THE ECLIPTIC (100–500 MEV)

Set of cuts in Figure 5	$\lvert\beta\rvert < 15°$ Flux, cm^{-2} s^{-1}	Stat. error	Fitted flux, cm^{-2} s^{-1}	Stat. error
a	1.006×10^{-5}	5.5×10^{-7}	9.16×10^{-6}	3.5×10^{-7}
b	7.95×10^{-6}	5.8×10^{-7}	5.95×10^{-6}	3.7×10^{-7}
c	3.59×10^{-6}	6.7×10^{-7}	3.53×10^{-6}	4.4×10^{-7}
d	1.1×10^{-7}	7.4×10^{-7}	1.52×10^{-6}	5.1×10^{-7}

Moskalenko, Porter, Digel, Michelson, & Ormes ApJ 681, 1708 (2008)

Connection of Heliosphere to ISM

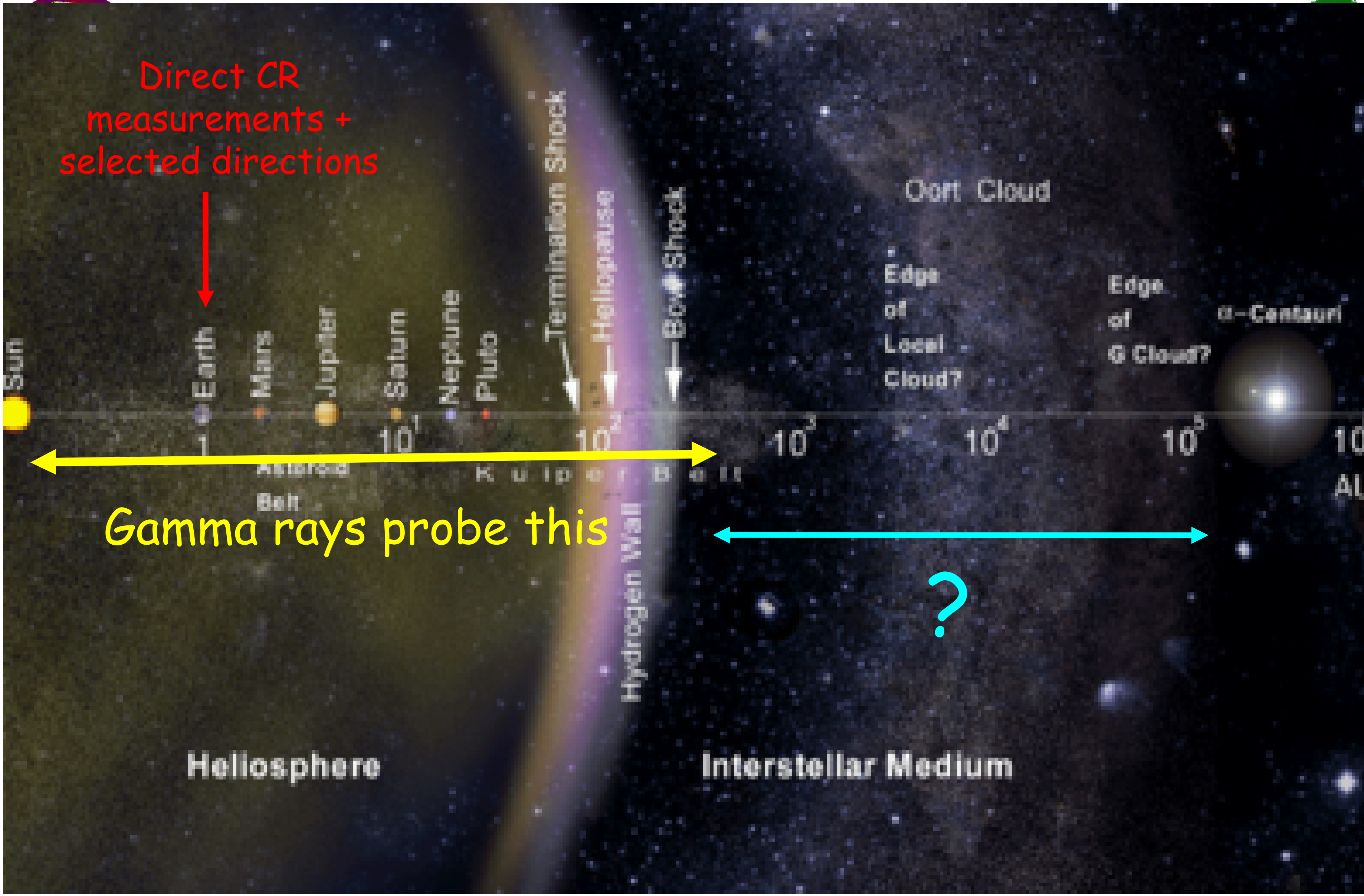

Propagation in the interstellar medium

A Model of CR Propagation in the Galaxy - GALPROP

- Gas distribution (energy losses, π^0, brems)
- Interstellar radiation field (IC, $e^{\pm}$ energy losses)
- Nuclear & particle production cross sections
- Gamma-ray production: brems, IC, π^0
- Energy losses: ionisation, Coulomb, brems, IC, synch
- Solve transport equations for all CR species
- Fix propagation parameters

How It Works: Fixing Propagation Parameters

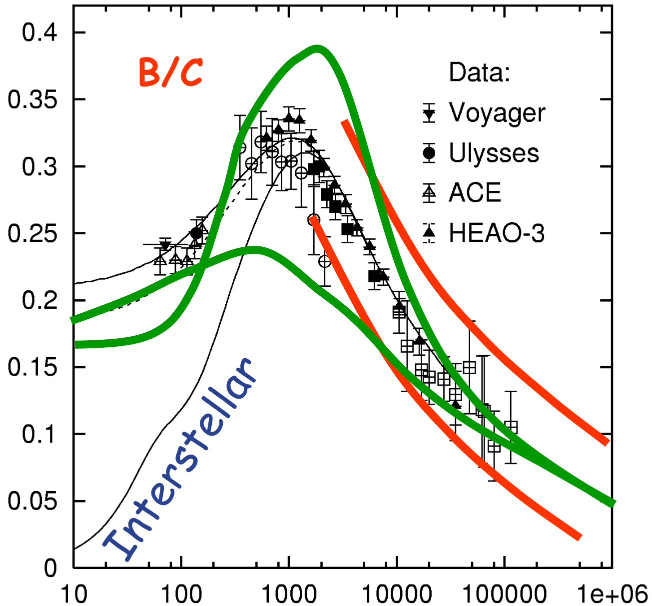

E_k, MeV/nucleon

Parameters (model dependent):

$D \sim 10^{28} (\rho/1\ GV)^{\alpha}\ cm^2/s$

$\delta \approx 0.3\text{-}0.6$

$Z_h \sim 4\text{-}6$ kpc

($V_A \sim 30$ km/s)

Diffusion coefficient

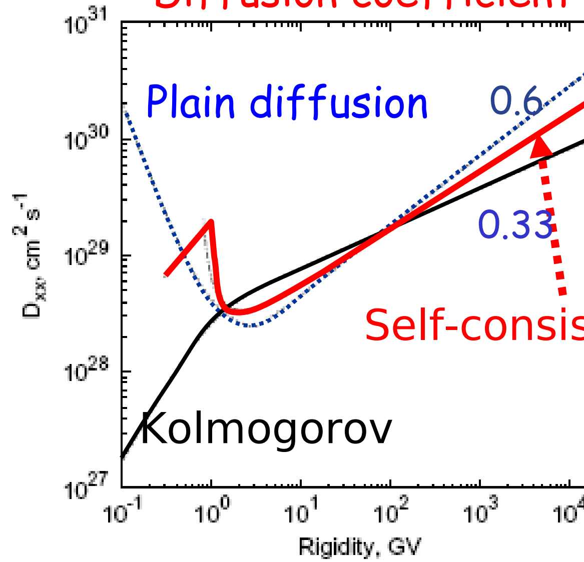

Using secondary/primary nuclei ratio & flux:

- Diffusion coefficient and its index
- Propagation mode and its parameters (e.g., reacceleration V_A, convection V_z)
- Propagation params are model-dependent
- Make sure that the spectrum is fitted as well

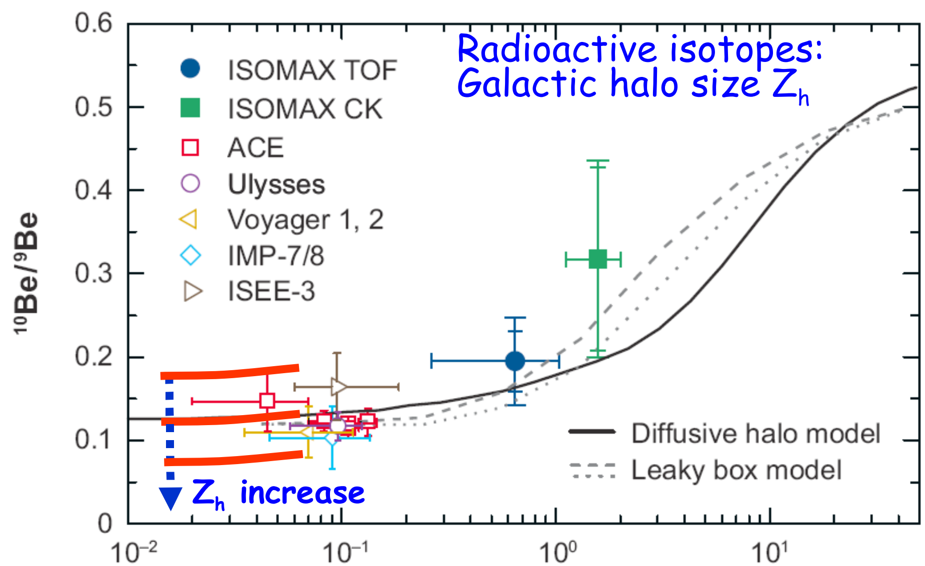

E_{kin}, GeV/nucleon

Discrimination of the propagation models

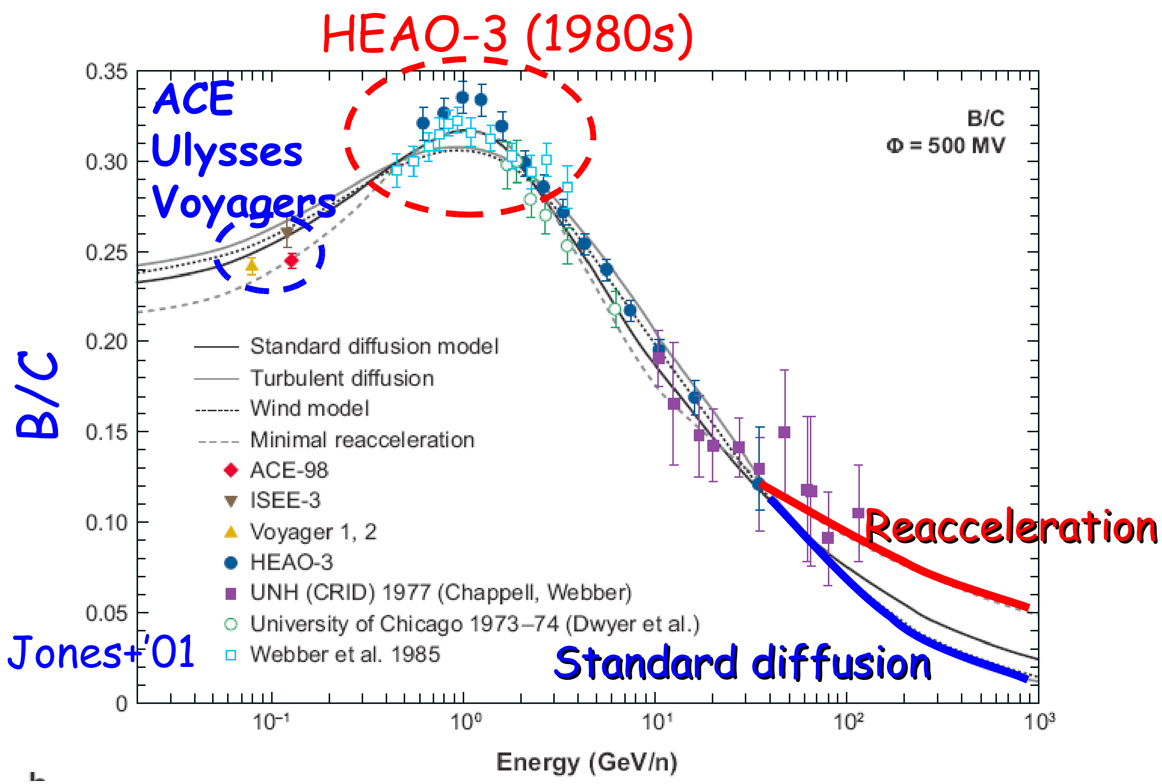

The data were taken at different times (1980-now) in different energy ranges and by different instruments, so the probability of systematic errors is high.

- Different propagation models are tuned to fit the low energy part of sec./prim. ratio where the accurate data exist
- However, the differ at high energies which will allow to discriminate between them when more accurate data will be available
- The sharp peak at ~1 GeV/nucleon seems to be confirmed by Pamela!

B/C from CREAM

Recent CREAM data extend B/C to ~ 1 TeV/n

- Antarctic balloon flight 2004/2005 summer (42 days), ~40 km altitude (~4 g cm^{-2})
- Pathlength distribution $\lambda \propto R^{-\delta}$
  - δ ~ 0.6, consistent with data < 30 GeV/n

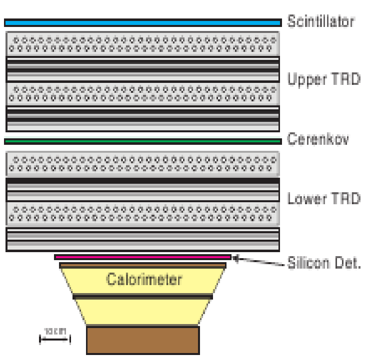

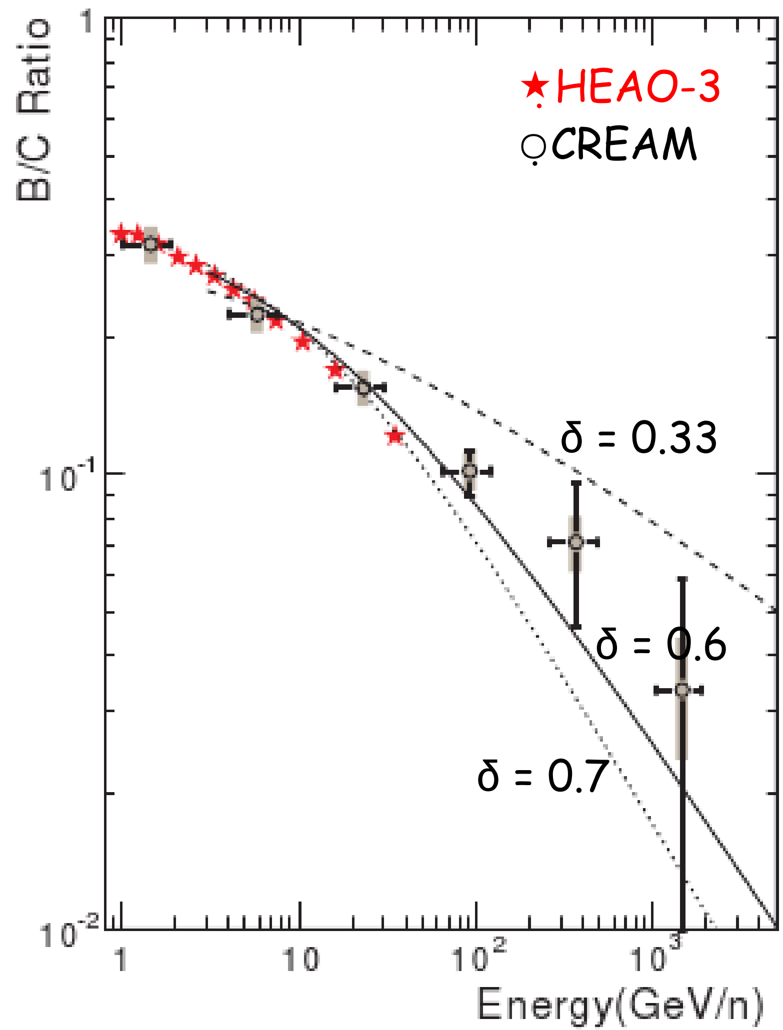

Ahn et al. (2008) arXiv:0808.1718

EGRET-Optimised model

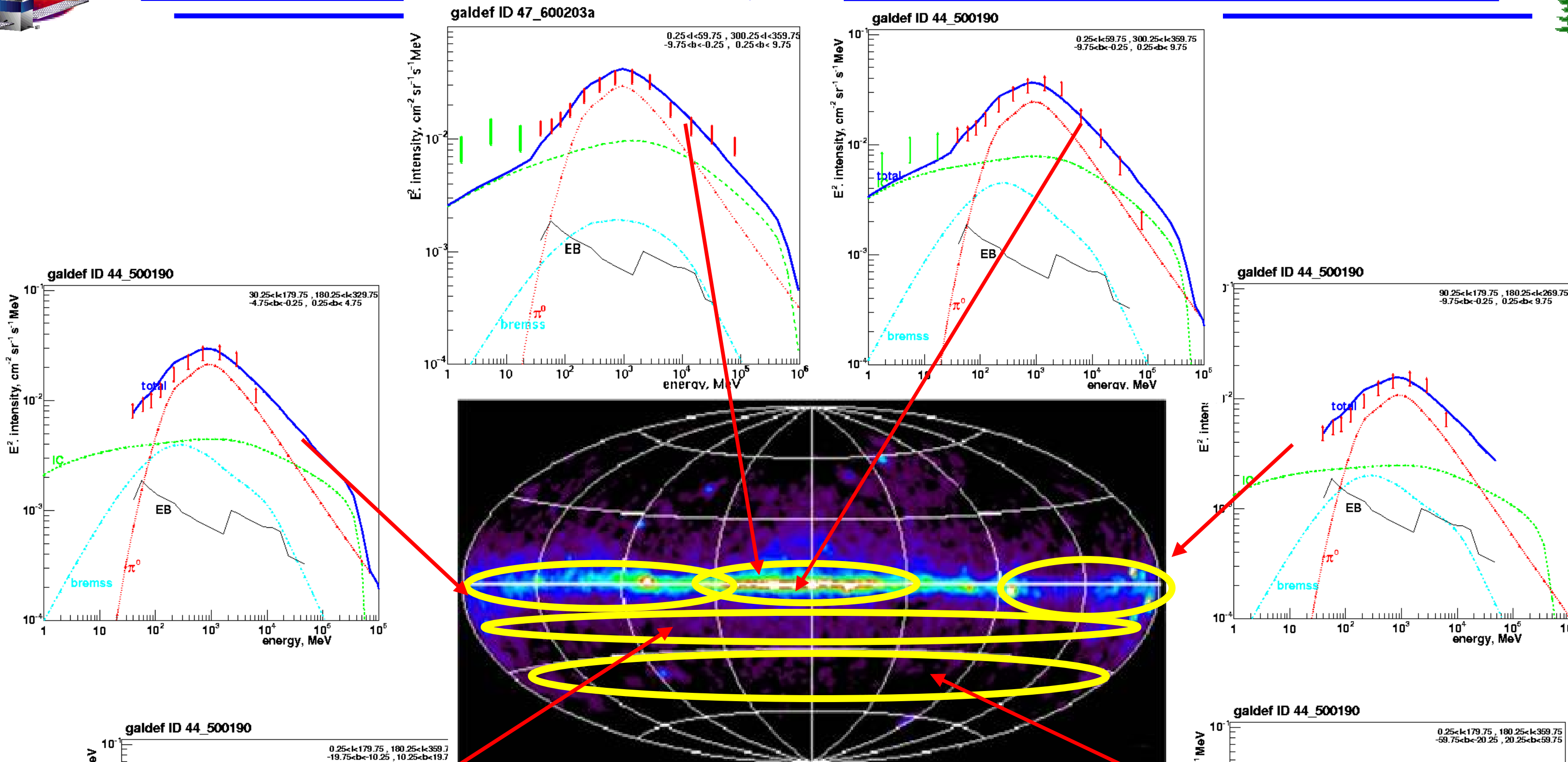

- CR spectra are not the same everywhere in the Galaxy
- Possible to tune proton and electron spectra to fit diffuse gamma rays

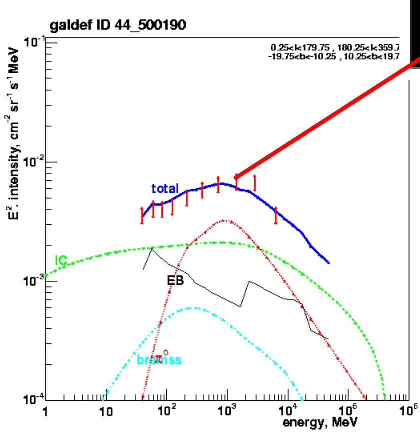

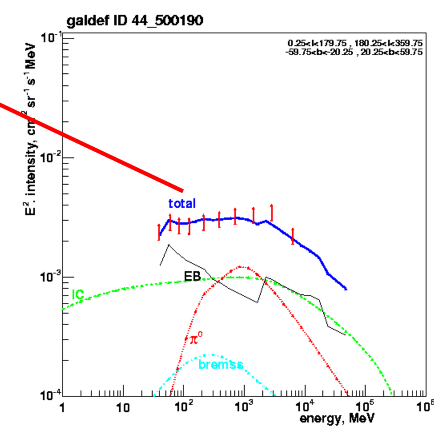

Strong+'00,'04

EGRET-Optimised/Reaccleration model

Uses all sky and antiprotons & gammas to fix the nucleon and electron spectra

- Uses antiprotons to fix the *intensity* of CR nucleons @ HE
- Uses gammas to adjust
  - the nucleon spectrum at LE
  - the *intensity* of the CR electrons

  (uses also synchrotron index)
- Uses EGRET data up to 100 GeV

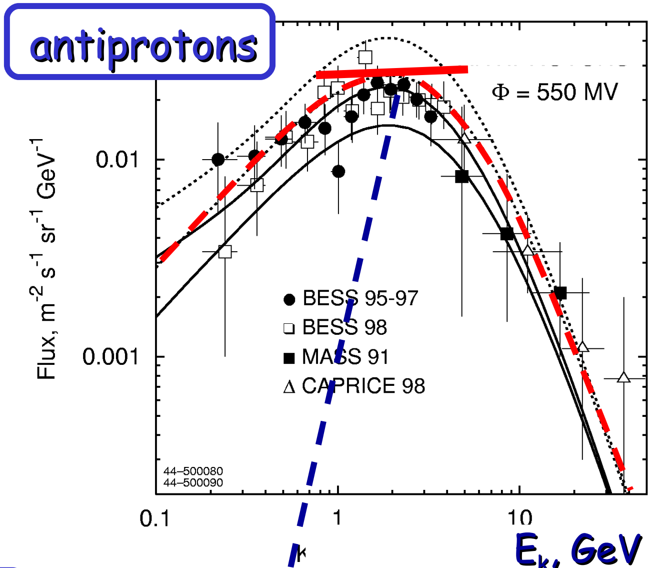

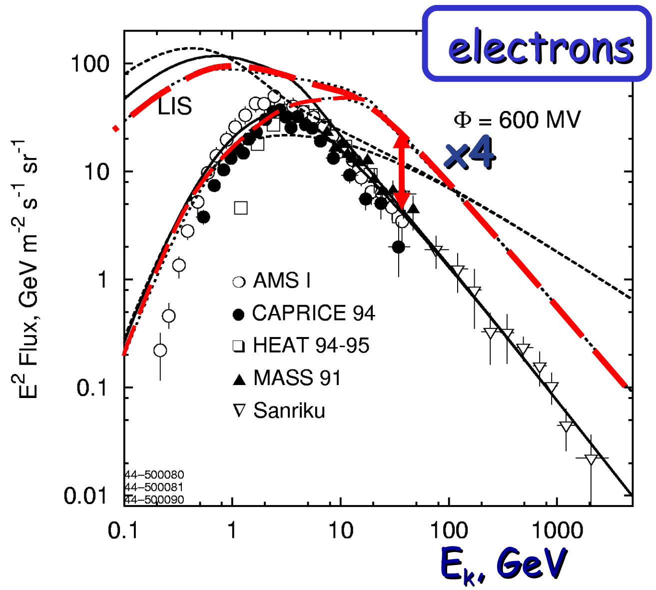

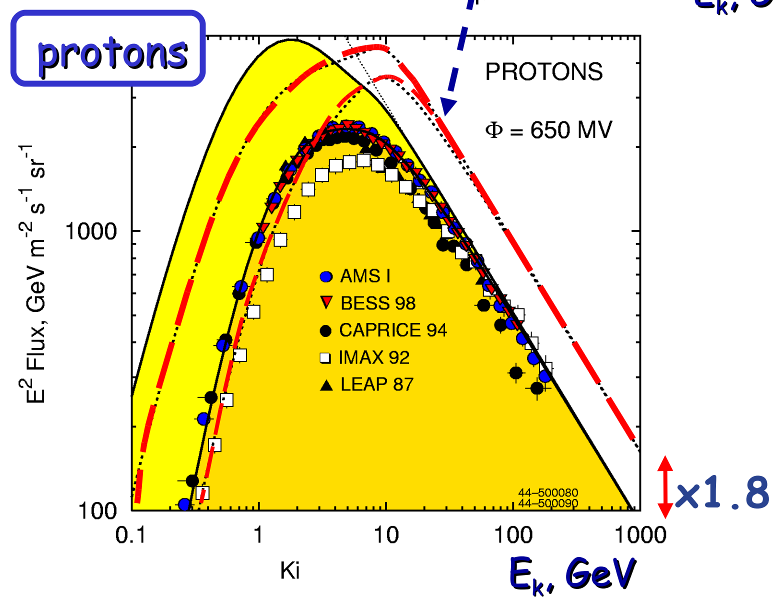

Fer

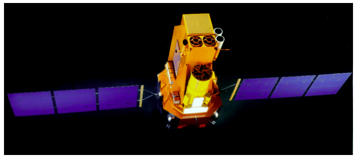

INTEGRAL / SPI Galactic emission

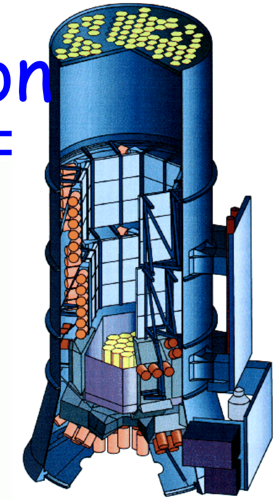

20 - 50 keV

50 - 100 keV

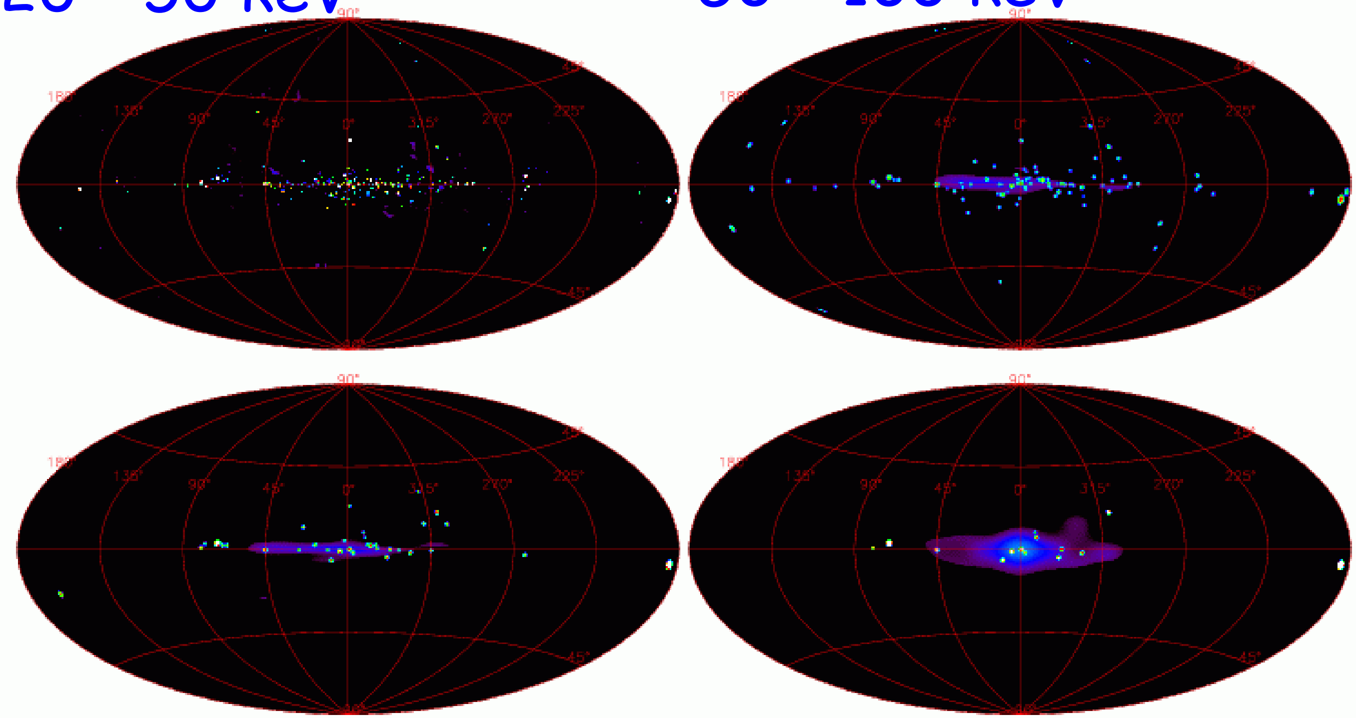

100 - 200 keV

200 - 600 keV

Bouchet et al 2008 ApJ 679,1315

CR Electrons and Positrons

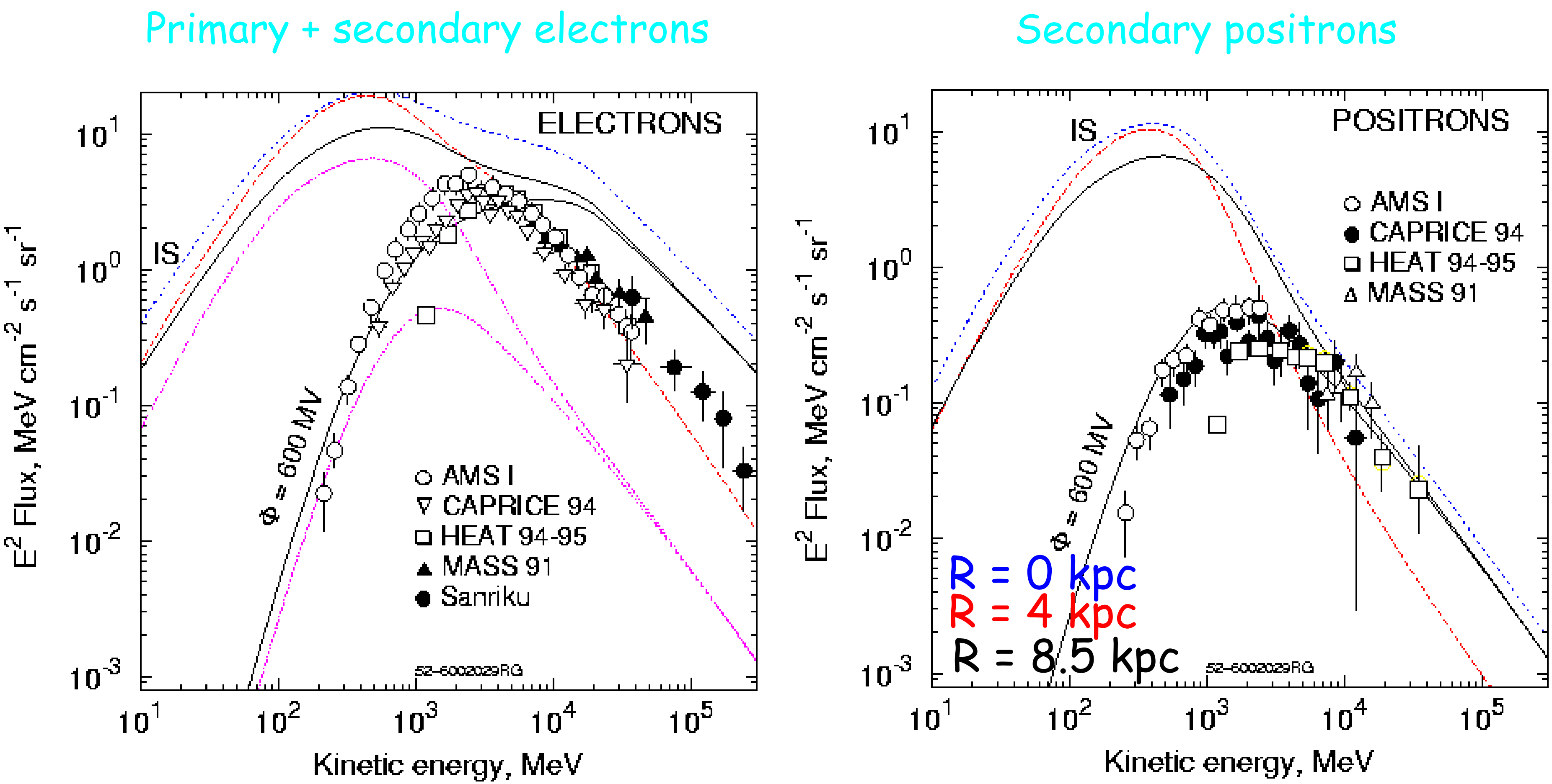

$pp \rightarrow \pi^{\pm} \rightarrow \mu^{\pm} \nu_{\mu} \rightarrow e^{\pm} \nu_{\mu} \nu_{e}$

Interstellar Radiation Field

- Emission by stars and reprocessing by dust
- MC radiative transfer calculation ⇒ self-consistent treatment
- Scale height ~10 kpc → ICS γs by CR $e^{\pm}$ in halo major component

Local ISRF

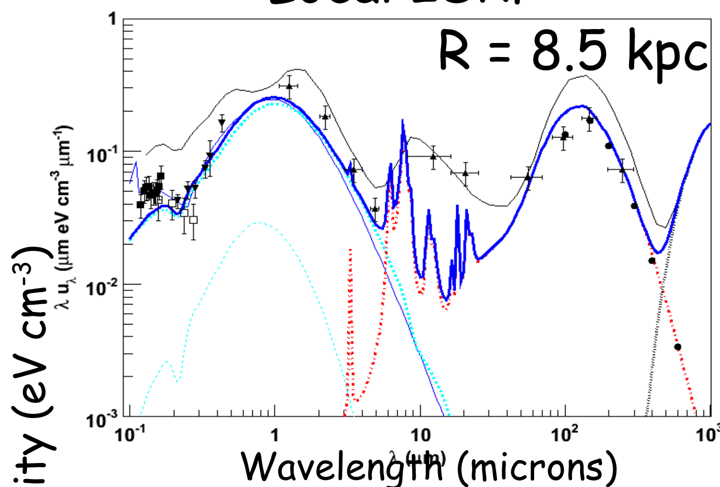

Galactic Plane ISRF

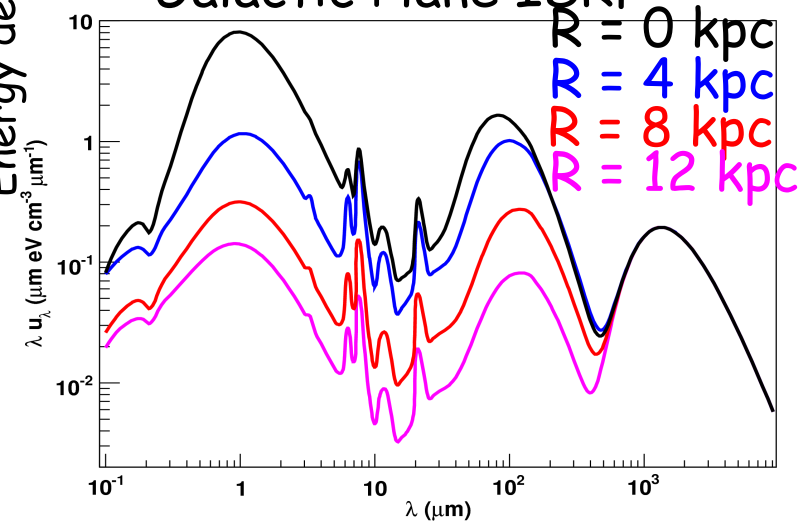

Total energy density

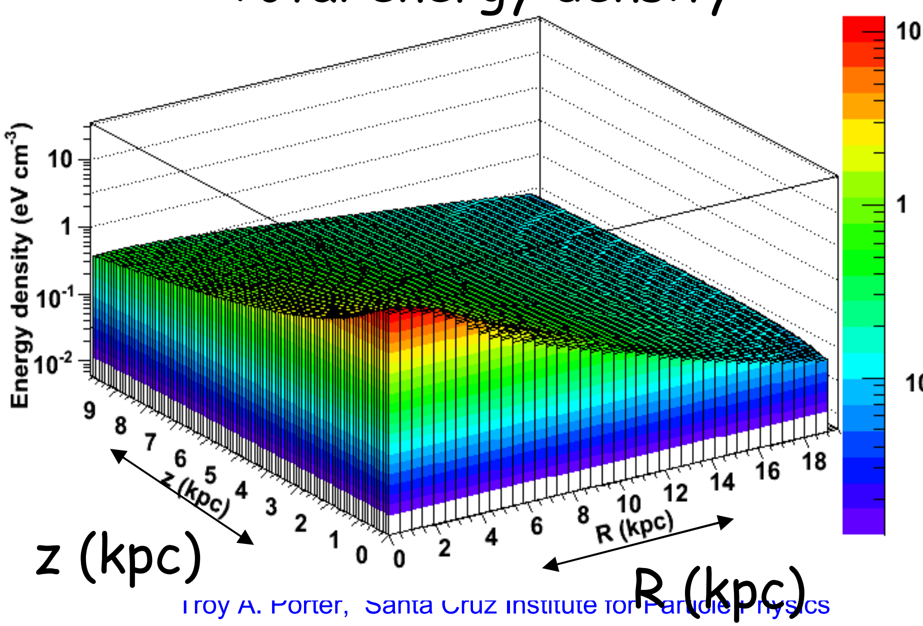

Gamma rays, inner Galaxy

IC = primary + secondary leptoons

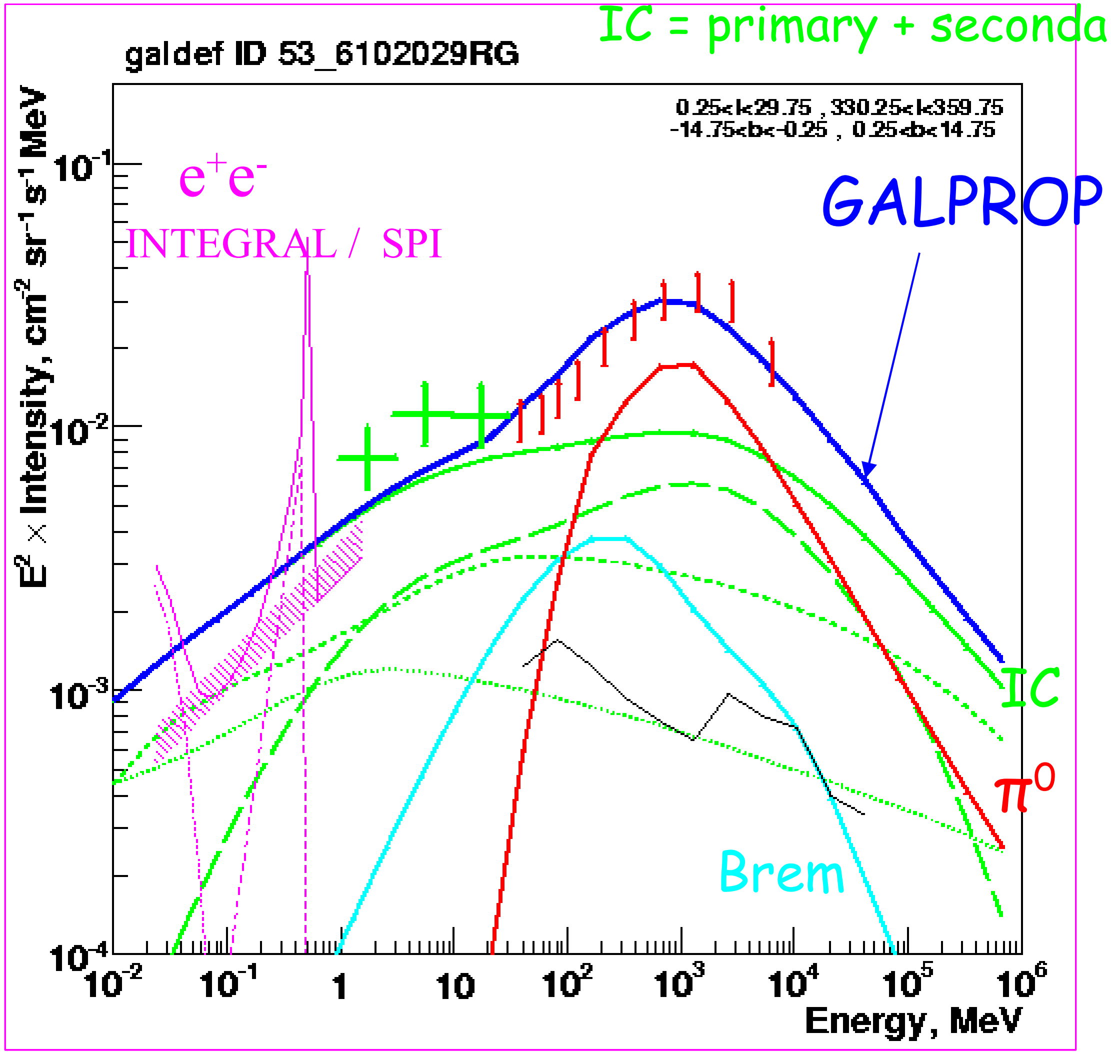

Porter, IVM, AWS, Orlando, & Bouchet ApJ 682, 400 (2008)

VHE Emission

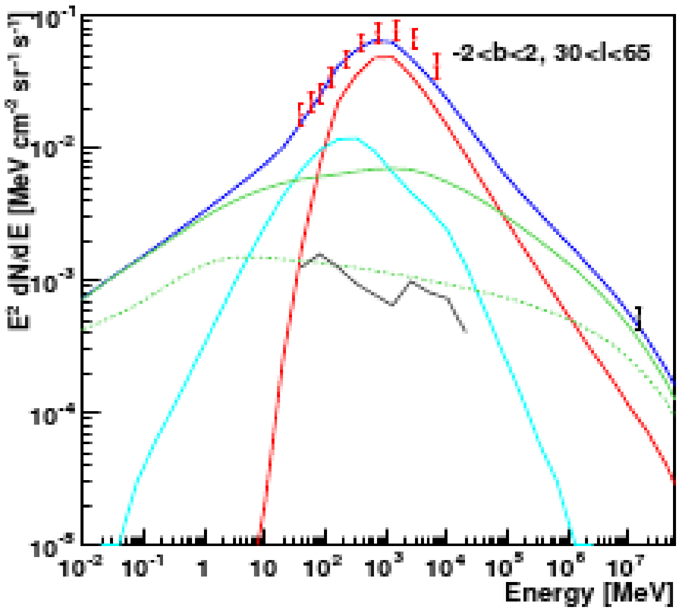

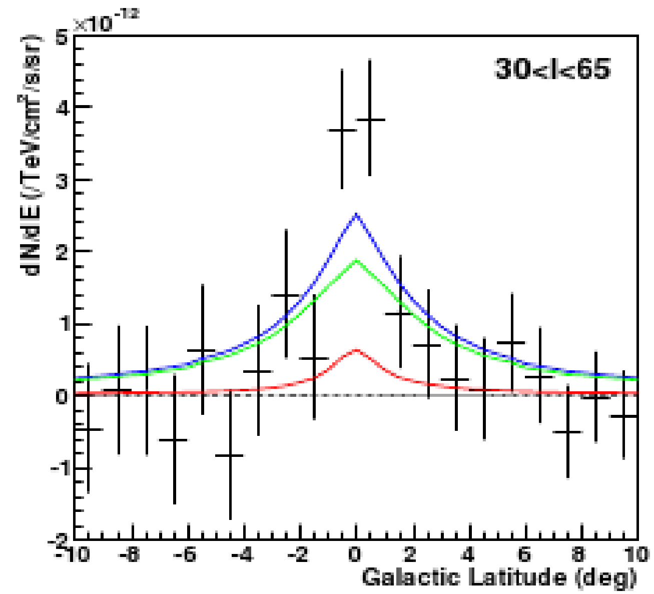

Fig.: Petra Hüntemeyer

Same model at MILAGRO energies

MILAGRO collab. + IVM, TAP, AWS ApJ in press (2008)

IC or π^0-decay?

Synchrotron Surveys

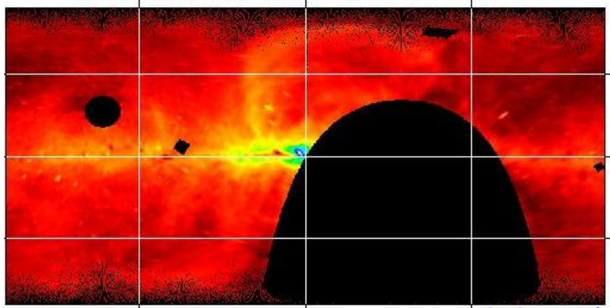

22 MHz

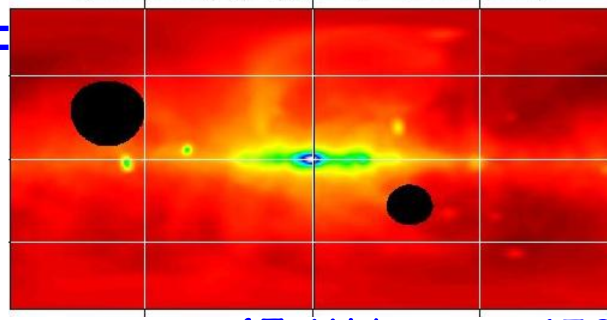

45 MHz

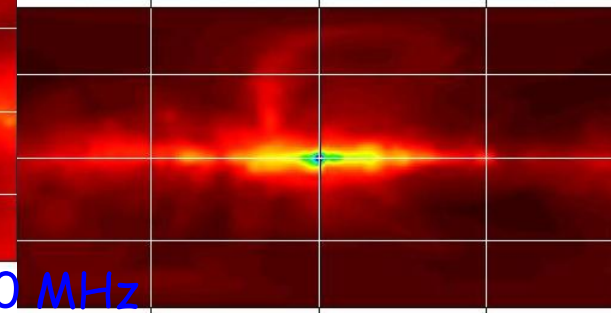

150 MHz

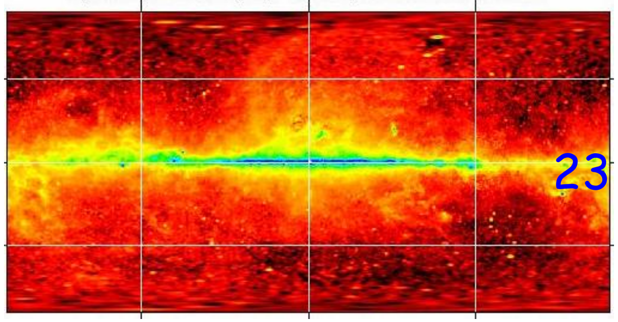

23 GHz

Continuum sky surveys

408 MHz

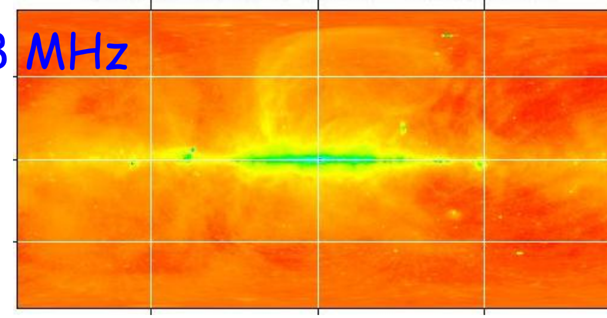

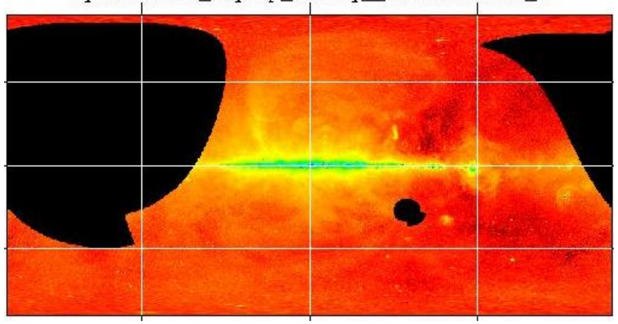

2.3 GHz

820 MHz

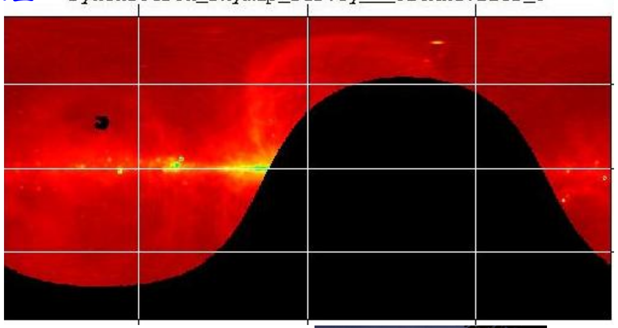

1.4 GHz

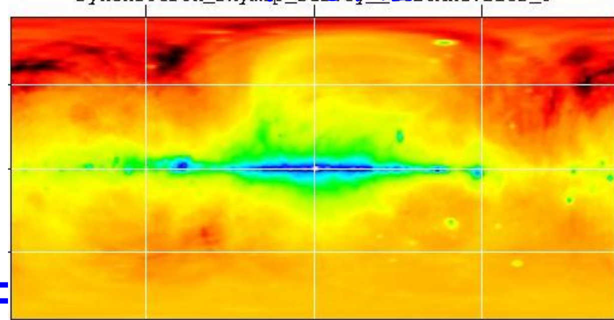

Radio Spectrum Northern Galaxy

Same model (optimised), random + reg B-field, electrons + positrons

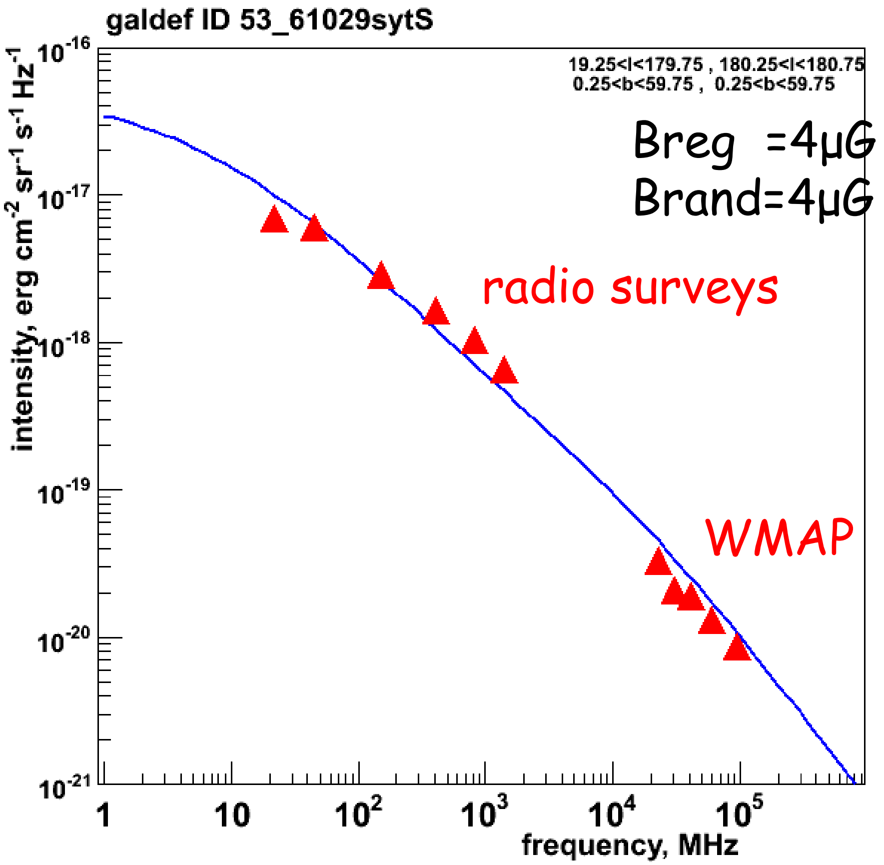

Model based on gamma-rays gives a good fit to the radio data

Interstellar Radiation over 20 Decades in Energy

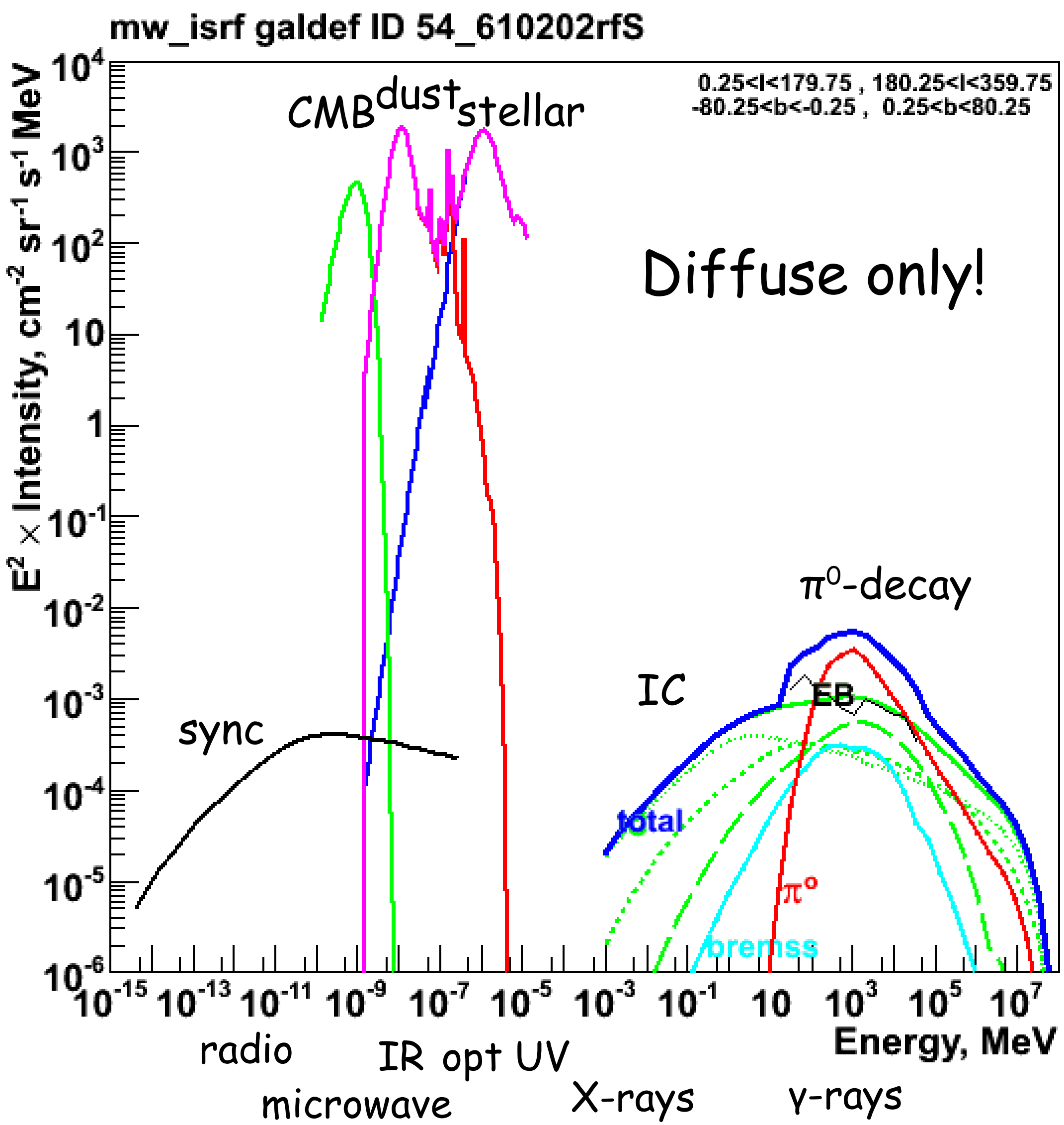

Interstellar Radiation over 20 Decades in Energy

Intrinsic connection between the diffuse Galactic γ-ray emission in different energy ranges:

- 100 keV - few MeV: IC emission by CR electrons and positrons on optical & IR radiation (primary + secondary electrons and positrons)
- 100 MeV - 10 GeV: produced by protons via π^0-decay; these protons also produce secondary positrons and electrons
- 10 GeV–10 TeV: Produced via IC scattering of primary electrons on the same optical & IR photons

Also same electrons and positrons synchrotron radiate off Galactic magnetic field → produce diffuse emission in MHz-GHz frequency range

Cosmic Rays in Other Galaxies: Magellanic Clouds

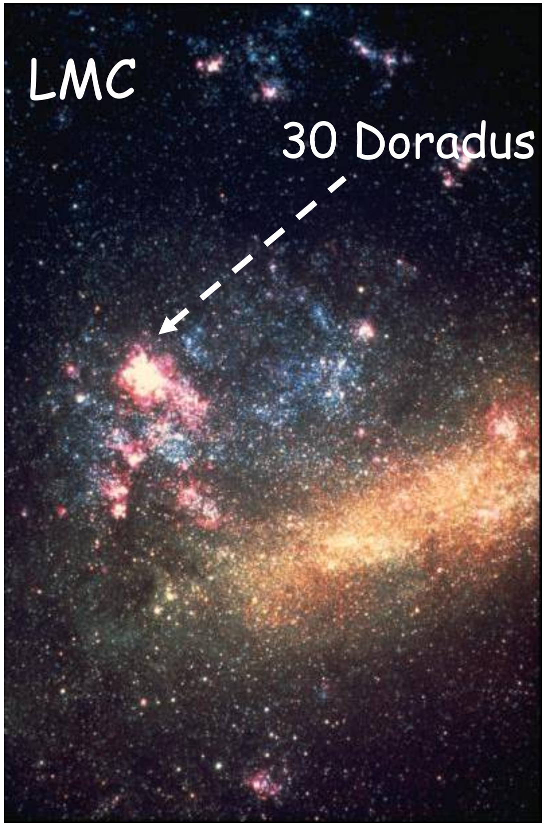

<u>Type:</u> Im IV-V
<u>Magnitude:</u> 2.3
<u>Size:</u> 280 x 160 arcmin <kpc
<u>Distance:</u> ~60 kpc

<u>Type:</u> Irr/SB(s)m
<u>Magnitude:</u> 0.9
<u>Size:</u> ~10°x10° ~few kpc
<u>Distance:</u> ~50 kpc

Summary: EGRET Observations

- LMC detection: CR density is similar to MW
- SMC non-detection: CR density is smaller than in the MW (otherwise it would be ~2.4×10^{-7} cm^{-2} s^{-1})
- First direct evidence:

  CRs are galactic and not universal !
- M31 non-detection: has to have smaller CR density than the MW (size M31>MW!)

Source	F(>100 MeV), cm^{-2} s^{-1}
LMC	$(1.9\pm0.4)\times10^{-7}$
SMC	$<0.5\times10^{-7}$
M31	$<0.8\times10^{-7}$

Sreekumar et al.(1992-94)

L_{MW}(>100 MeV)~5.4×10^{39} erg/s (SMR00)

~3×10^{43} phot/s

F_{MW}(@M31 distance) ~ 4.4×10^{-7}cm^{-2} s^{-1}

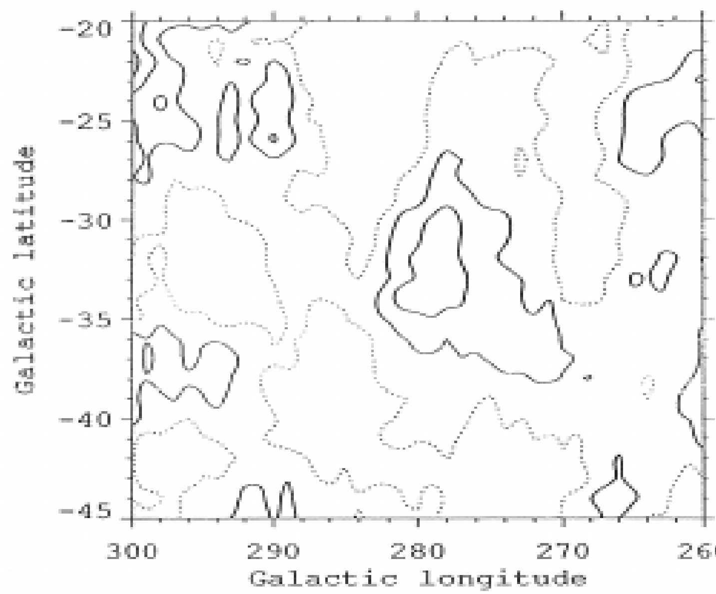

FIG. 1.—Contour plot (slightly smoothed for clarity) of observed intensity from the LMC region (combined data from the two observations) after background subtraction. The contour levels (0, 5, 10) are in units of 10^{-6} photons (E > 100 MeV) cm^{-2} s^{-1} sr^{-1}. The spatial extent is consistent with that seen at radio frequencies (l ~ 275°–282°; b ~ −37° to −30°). Additional small regions seen at the 5 × 10^{-6} level are not statistically significant.

LMC: Sreekumar et al. '92

Fermi LAT Project

Extragalactic Gamma-Ray Background

Predicted vs. observed

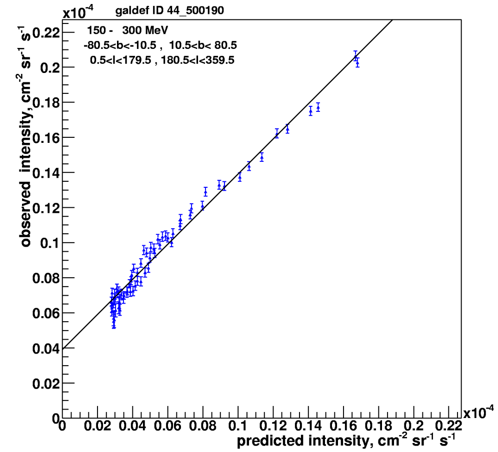

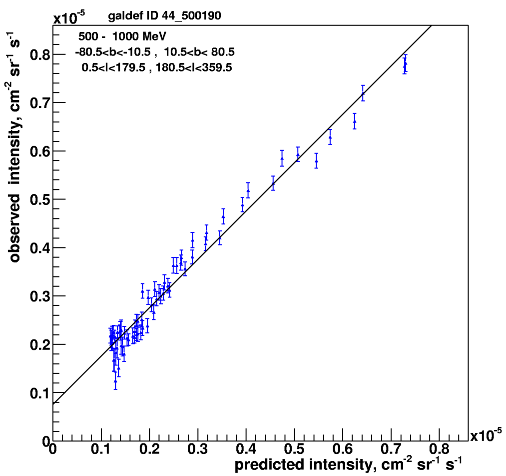

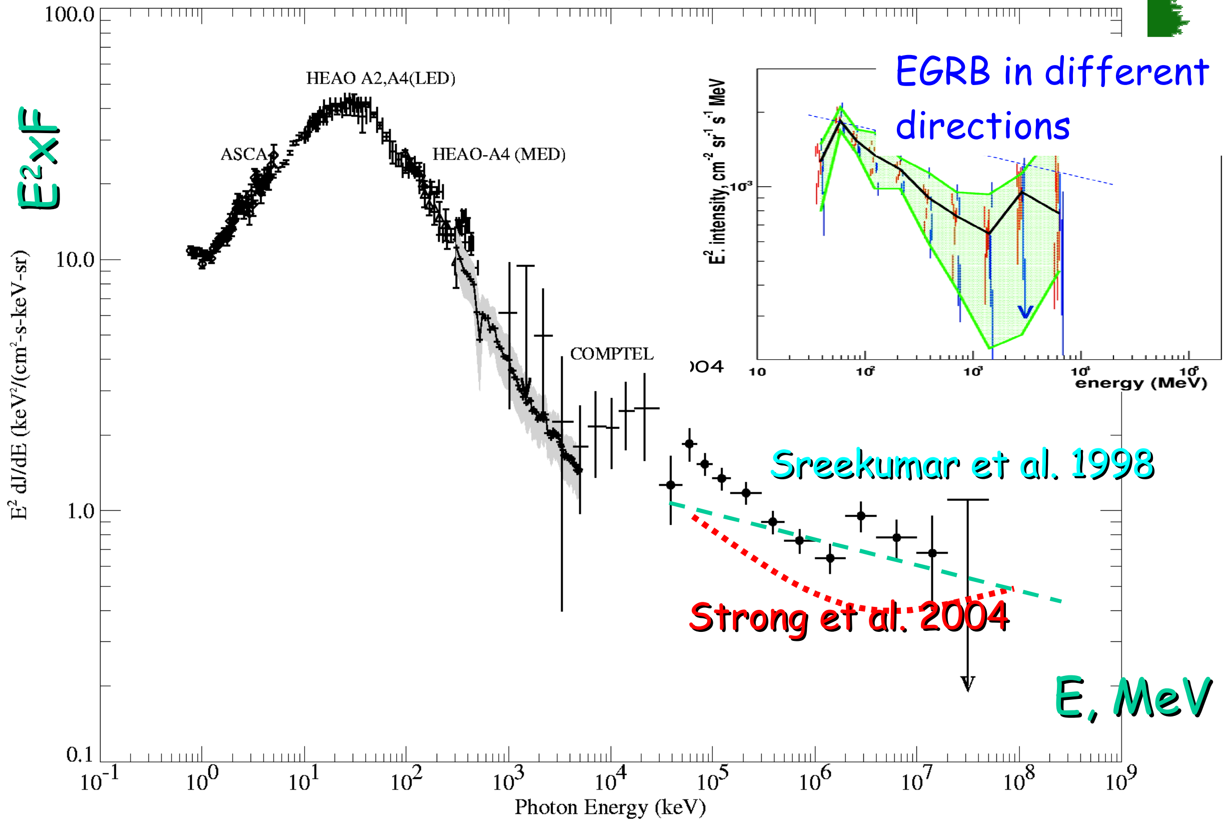

Extragalactic Gamma-Ray Background

Predicted vs. observed

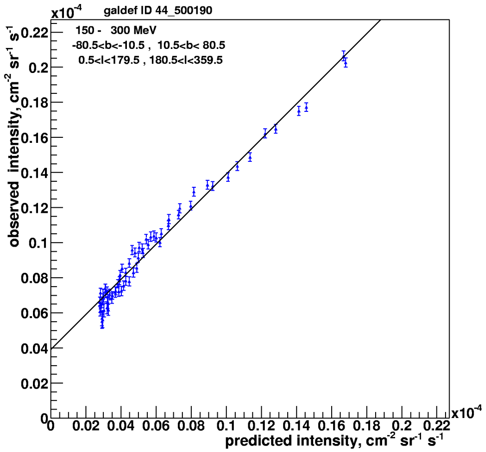

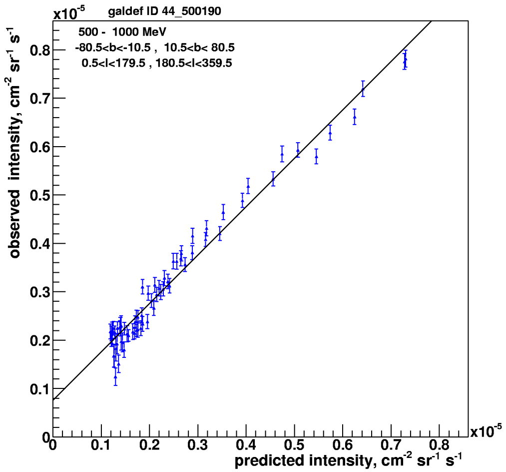

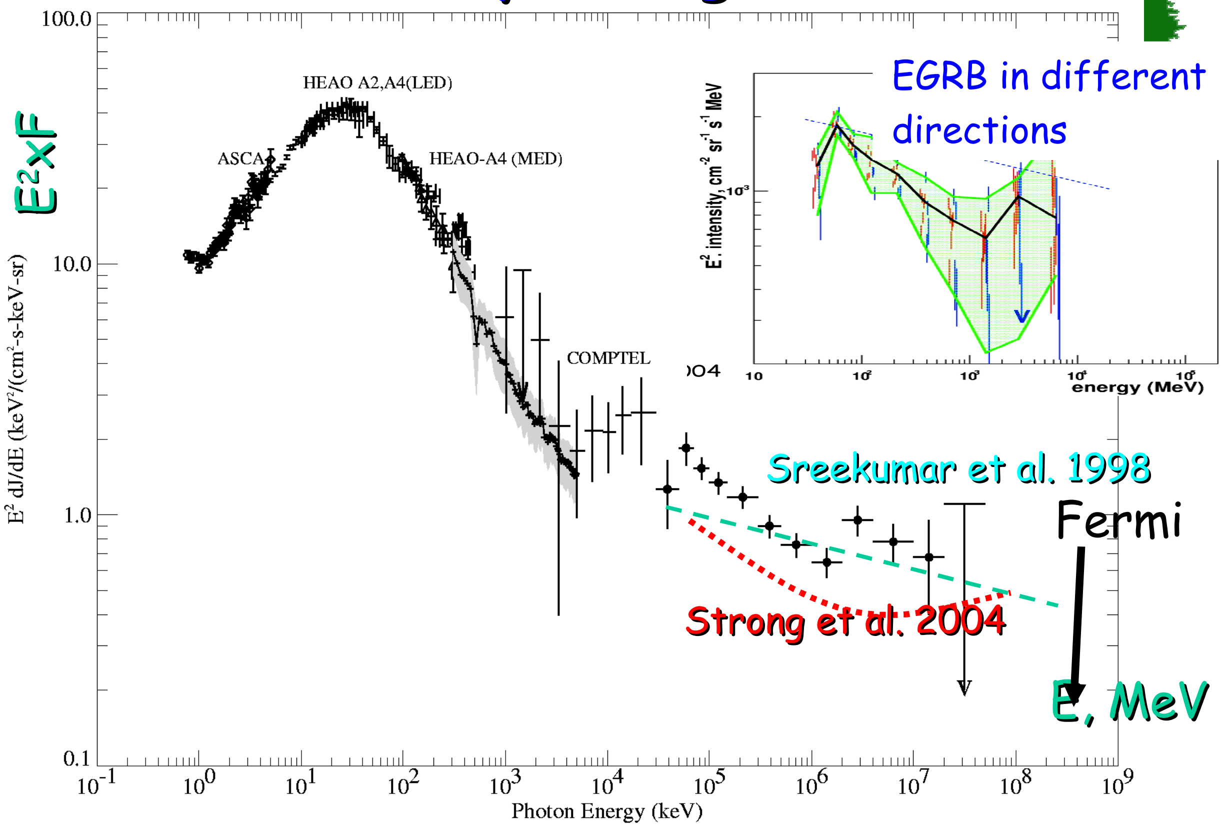

Extragalactic Gamma-Ray Background

Predicted vs. observed

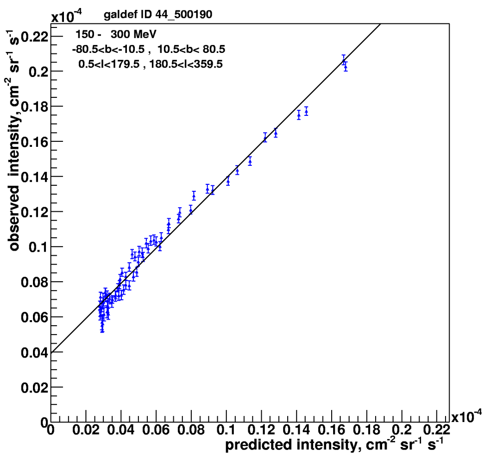

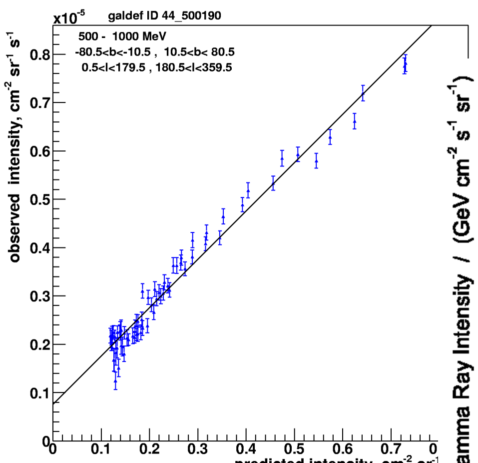

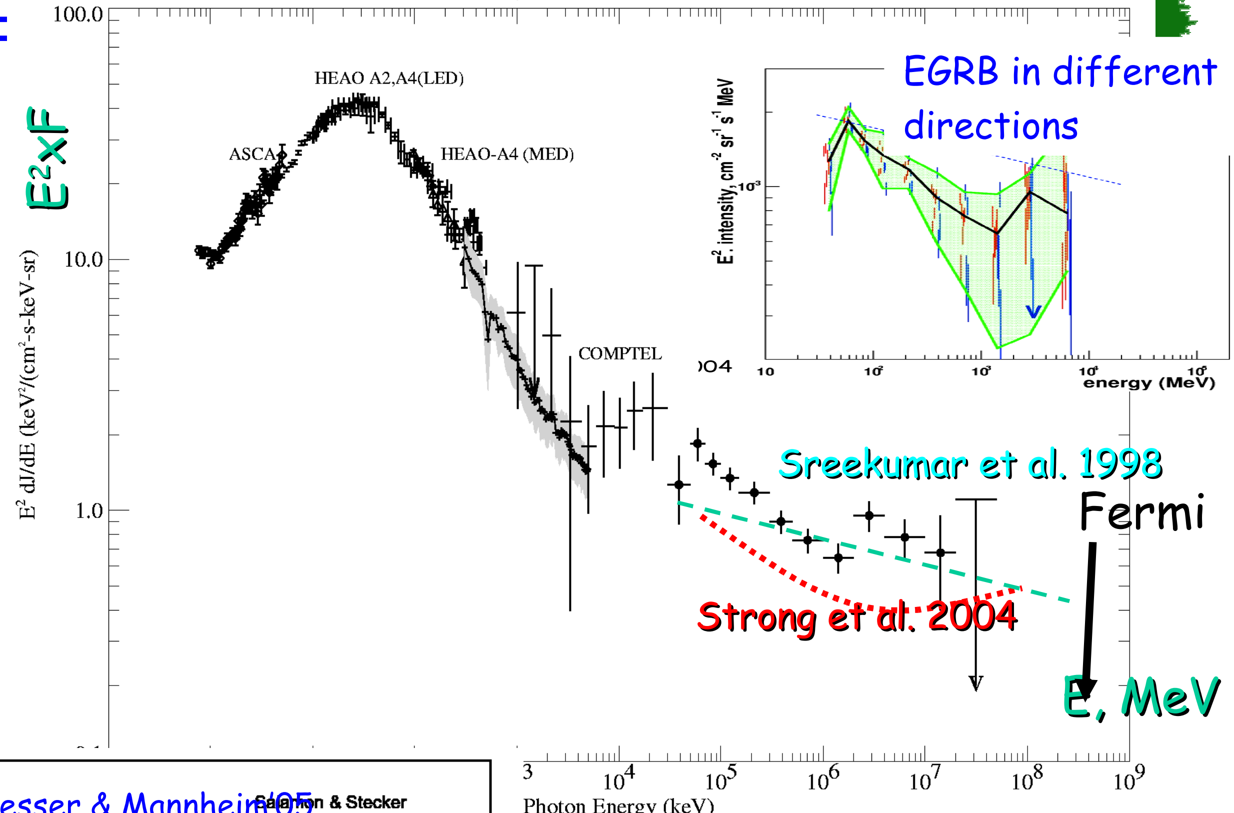

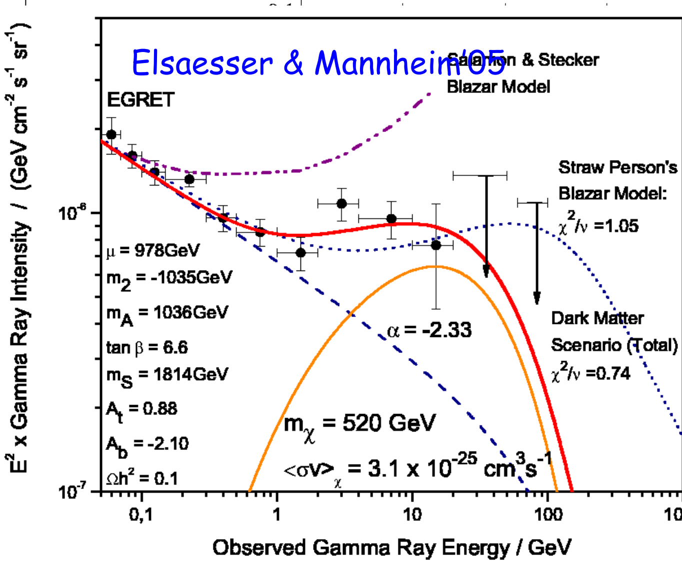

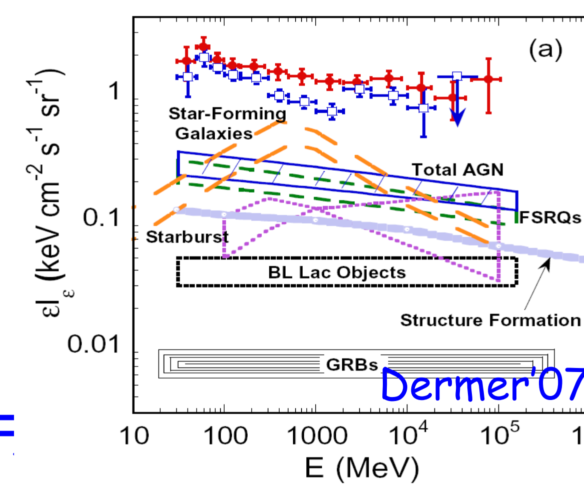

Examples of Dark Matter Signatures in CRs

Diffuse gammas

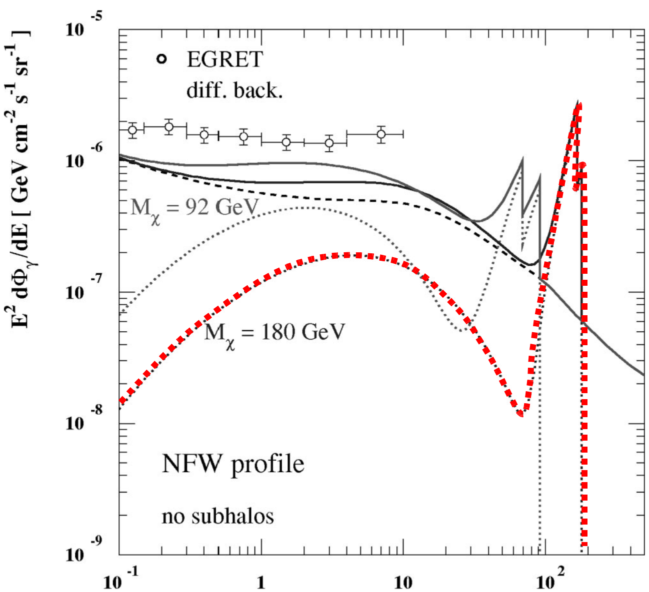

E, GeV

Antiprotons

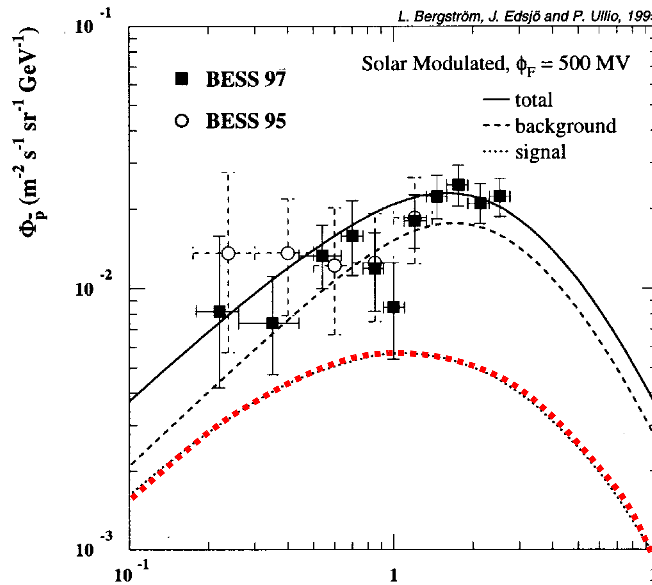

E_k, GeV

Look for a consistent signal in diffuse gamma rays, and CRs (antiprotons, antideuterons, positrons)

Fermi LAT Project

Positrons

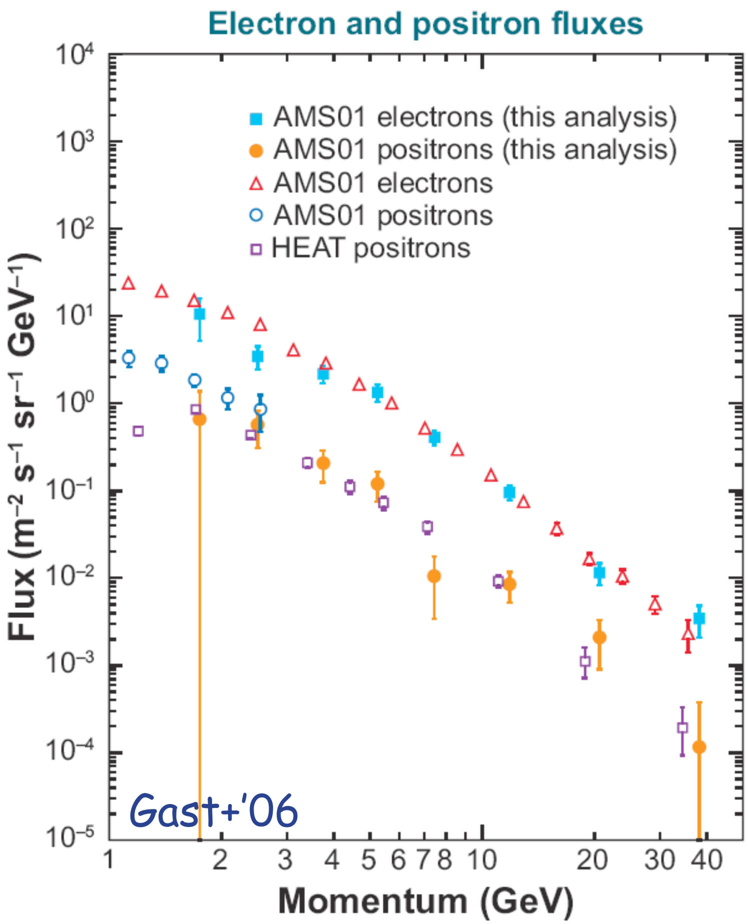

Positron flux is consistent with predictions, but the error bars are large

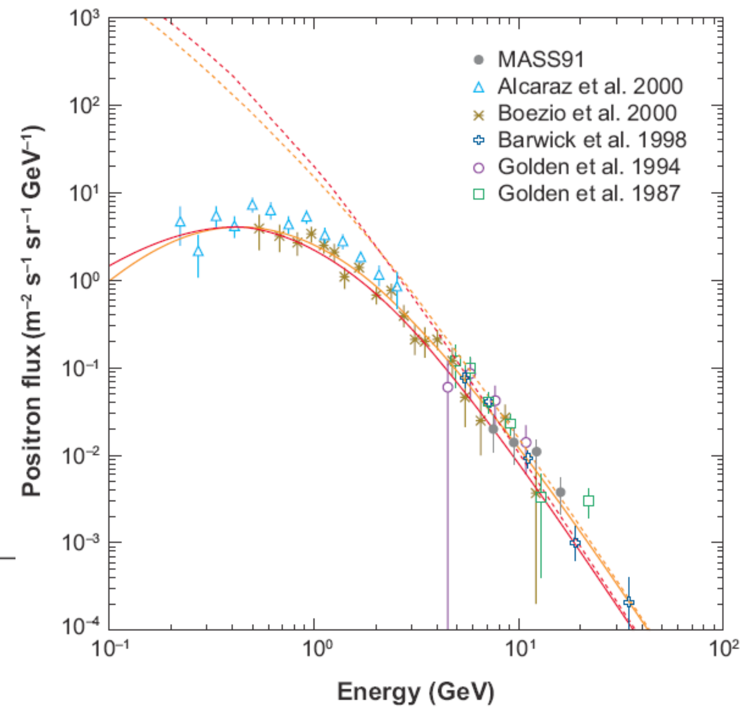

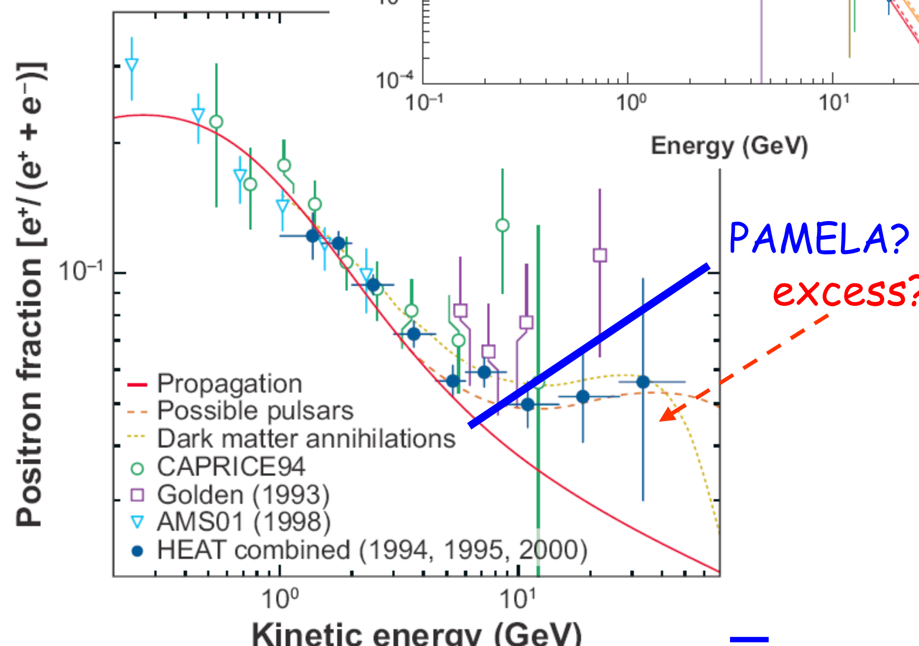

The "haze" at the Galactic Centre (WMAP)

Synchrotron emission from leptons produced in WIMP annihilations?

Dark Matter in the WMAP Sky

- In 2004, Doug Finkbeiner suggested that the WMAP Haze could be synchtrotron from electrons/positrons produced in dark matter annihilations in the inner galaxy (astro-ph/0409027)

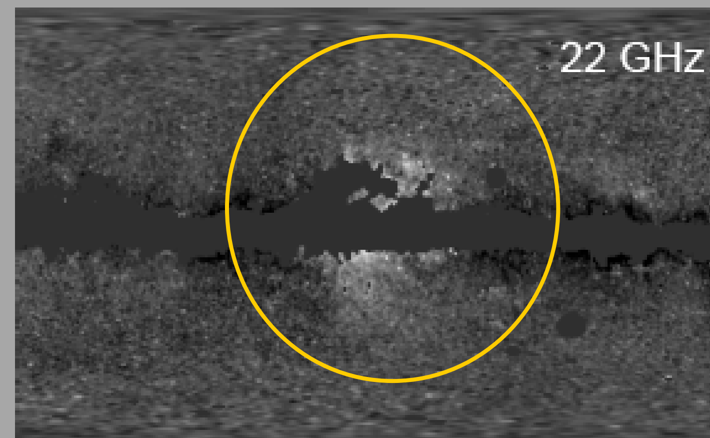

- In particular, he noted that:

1) Assuming an NFW profile, a WIMP mass of 100 GeV and an annihilation cross section of 3×10^{-26} cm^3/s, the total power in dark matter annihilations in the inner 3 kpc of the Milky Way is

~1.2×10^{39} GeV/sec

Coincidence?

2) The total power of the WMAP Haze is between

0.7×10^{39} and 3×10^{39} GeV/sec

Dan Hooper - *Dark Matter Annihilations in the WMAP Sky*

Summary

- We are making progress toward directly connecting the CR spectra we see in the heliosphere to the interstellar medium
- We are also developing a multi-wavelength picture of the diffuse emission from standard astrophysical processes
- Both of these are crucial for understanding many current topics
- We look forward to data to come from PAMELA, Fermi-LAT, and other instruments – this is a very exciting time for cosmic rays physics!

Cosmology

- Synchrotron + dust emission important foreground for CMB experiments
- Provide important information about GMF

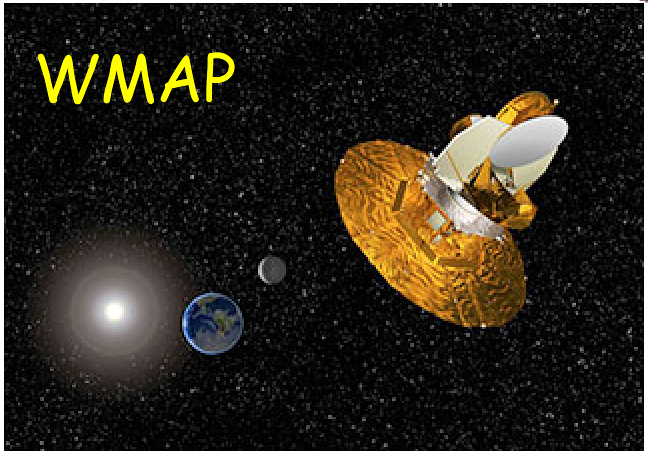

Kogut et al 2007: WMAP polarised index 22-33 GHz

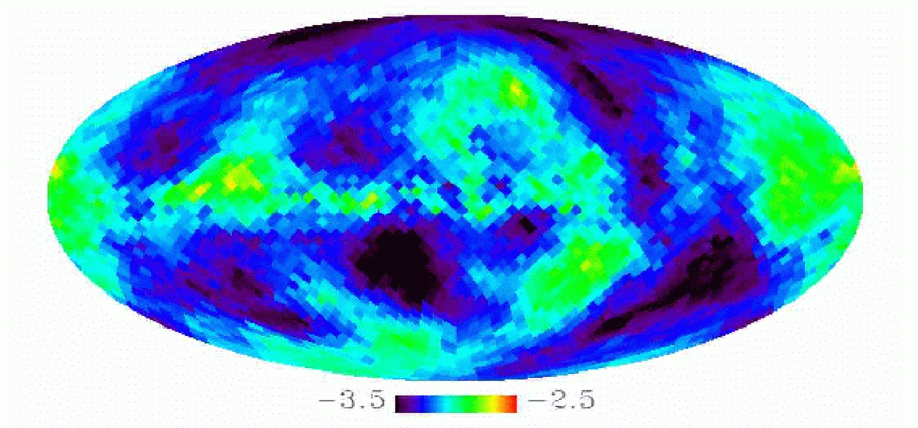

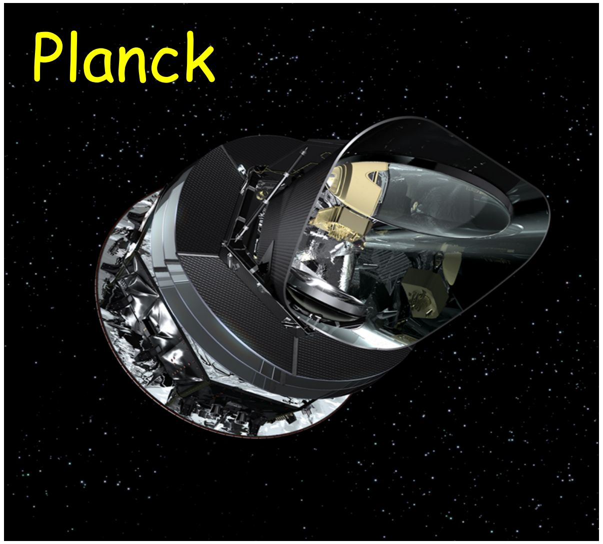

Ultra High Energy CRs

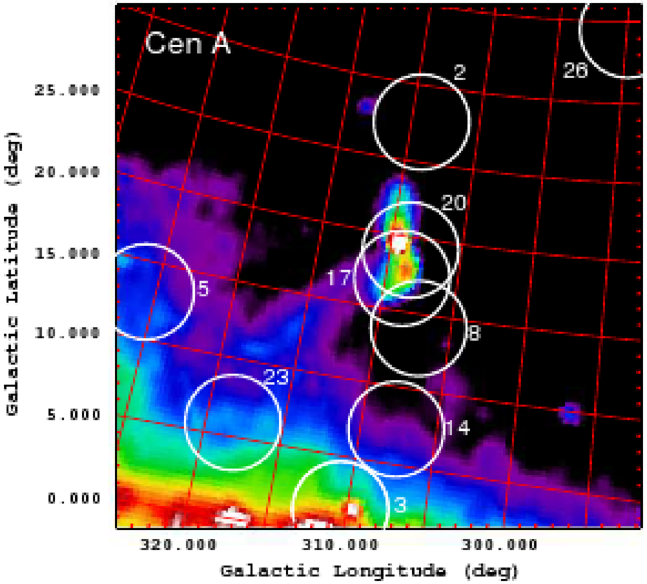

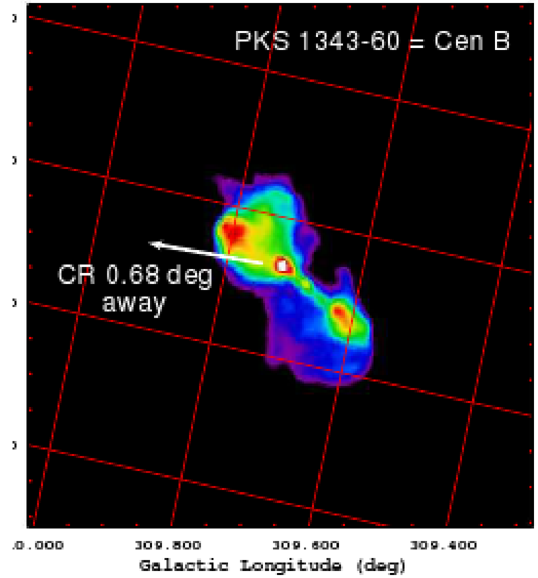

IVM, Stawarz, Porter, & Cheung arXiv:0805.1260

Pierre Auger Collab. '07,'08

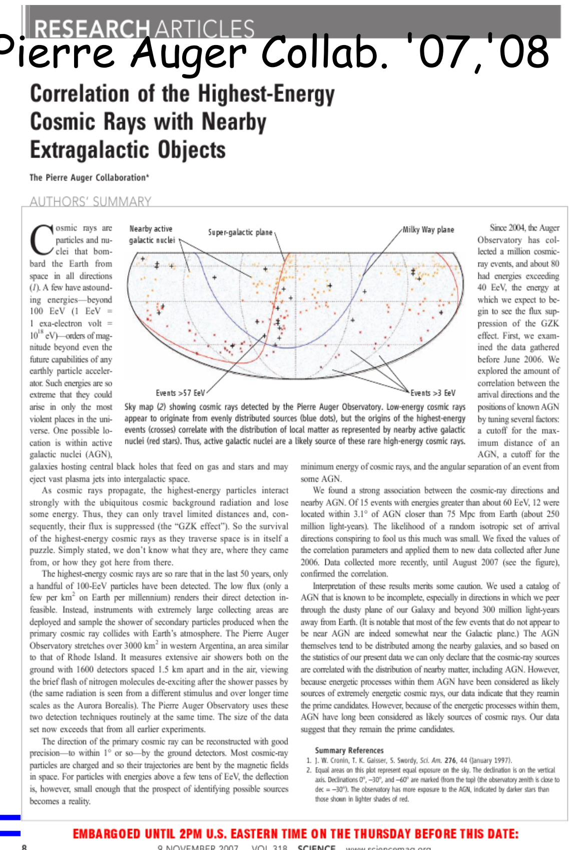

RESEARCH ARTICLES

Correlation of the Highest-Energy Cosmic Rays with Nearby Extragalactic Objects

The Pierre Auger Collaboration*

AUTHORS' SUMMARY

Cosmic rays are particles and nuclei that bombard the Earth from space in all directions (1). A few have astounding energies—beyond 100 EeV (1 EeV = 1 exa-electron volt = 10^{18} eV)—orders of magnitude beyond even the future capabilities of any earthly particle accelerator. Such energies are so extreme that they could arise in only the most violent places in the universe. One possible location is within active galactic nuclei (AGN), galaxies hosting central black holes that feed on gas and stars and may eject vast plasma jets into intergalactic space.

As cosmic rays propagate, the highest-energy particles interact strongly with the ubiquitous cosmic background radiation and lose some energy. Thus, they can only travel limited distances and, consequently, their flux is suppressed (the "GZK effect"). So the survival of the highest-energy cosmic rays as they traverse space is in itself a puzzle. Simply stated, we don't know what they are, where they came from, or how they got here from there.

The highest-energy cosmic rays are so rare that in the last 50 years, only a handful of 100-EeV particles have been detected. The low flux (only a few per km^2 on Earth per millennium) renders their direct detection infeasible. Instead, instruments with extremely large collecting areas are deployed and sample the shower of secondary particles produced when the primary cosmic ray collides with Earth's atmosphere. The Pierre Auger Observatory stretches over 3000 km^2 in western Argentina, an area similar to that of Rhode Island. It measures extensive air showers both on the ground with 1600 detectors spaced 1.5 km apart and in the air, viewing the brief flash of nitrogen molecules de-exciting after the shower passes by (the same radiation is seen from a different stimulus and over longer time scales as the Aurora Borealis). The Pierre Auger Observatory uses these two detection techniques routinely at the same time. The size of the data set now exceeds that from all earlier experiments.

The direction of the primary cosmic ray can be reconstructed with good precision—to within 1° or so—by the ground detectors. Most cosmic-ray particles are charged and so their trajectories are bent by the magnetic fields in space. For particles with energies above a few tens of EeV, the deflection is, however, small enough that the prospect of identifying possible sources becomes a reality.

Nearby active galactic nuclei
Super-galactic plane
Milky Way plane
Events >57 EeV
Events >3 EeV

Sky map (2) showing cosmic rays detected by the Pierre Auger Observatory. Low-energy cosmic rays appear to originate from evenly distributed sources (blue dots), but the origins of the highest-energy events (crosses) correlate with the distribution of local matter as represented by nearby active galactic nuclei (red stars). Thus, active galactic nuclei are a likely source of these rare high-energy cosmic rays.

Since 2004, the Auger Observatory has collected a million cosmic-ray events, and about 80 had energies exceeding 40 EeV, the energy at which we expect to begin to see the flux suppression of the GZK effect. First, we examined the data gathered before June 2006. We explored the amount of correlation between the arrival directions and the positions of known AGN by tuning several factors: a cutoff for the maximum distance of an AGN, a cutoff for the minimum energy of cosmic rays, and the angular separation of an event from some AGN.

We found a strong association between the cosmic-ray directions and nearby AGN. Of 15 events with energies greater than about 60 EeV, 12 were located within 3.1° of AGN closer than 75 Mpc from Earth (about 250 million light-years). The likelihood of a random isotropic set of arrival directions conspiring to fool us this much was small. We fixed the values of the correlation parameters and applied them to new data collected after June 2006. Data collected more recently, until August 2007 (see the figure), confirmed the correlation.

Interpretation of these results merits some caution. We used a catalog of AGN that is known to be incomplete, especially in directions in which we peer through the dusty plane of our Galaxy and beyond 300 million light-years away from Earth. (It is notable that most of the few events that do not appear to be near AGN are indeed somewhat near the Galactic plane.) The AGN themselves tend to be distributed among the nearby galaxies, and so based on the statistics of our present data we can only declare that the cosmic-ray sources are correlated with the distribution of nearby matter, including AGN. However, because energetic processes within them AGN have been considered as likely sources of extremely energetic cosmic rays, our data indicate that they reamin the prime candidates. However, because of the energetic processes within them, AGN have long been considered as likely sources of cosmic rays. Our data suggest that they remain the prime candidates.

Summary References
1. J. W. Cronin, T. K. Gaisser, S. Swordy, *Sci. Am.* **276**, 44 (January 1997).
2. Equal areas on this plot represent equal exposure on the sky. The declination is on the vertical axis. Declinations 0°, –30°, and –60° are marked (from the top) (the observatory zenith is close to dec = –30°). The observatory has more exposure to the AGN, indicated by darker stars than those shown in lighter shades of red.

EMBARGOED UNTIL 2PM U.S. EASTERN TIME ON THE THURSDAY BEFORE THIS DATE:

8 9 NOVEMBER 2007 VOL 318 SCIENCE www.sciencemag.org

- GMF → propagation of UHECRs from sources near Galactic plane
- Association with the sources of UHECRs